

Evaluation of Matrix Elements from a Graphical Representation of the Angular Integral*

JOHN S. BRIGGS†

Department of Physics, University of Chicago, Chicago, Illinois 60637

Argonne National Laboratory, Argonne, Illinois 60439

The graphical representation of angular momentum is used as the basis of a procedure for the complete evaluation of the matrix element of a Coulomb or multipole interaction operator between atomic states having any number of open shells. The method is presented in the form of a step-by-step procedure and is designed to permit straightforward extension to the evaluation of the matrix elements of other types of tensor operators and of sums of products of Coulomb matrix elements, such as occur in the perturbation theory of configuration interaction.

CONTENTS

1. Introduction.....	189
2. Graphical Representation.....	191
2.1 The Interaction Operators.....	191
2.2 Many-Electron Wave Functions.....	193
2.3 Fractional Parentage Expansion.....	194
3. The Coulomb Matrix Element.....	195
3.1 Integration over Electron Variables.....	195
3.2 Phase Factor and Weight Factor.....	196
4. Evaluation of the Angular Factor.....	199
4.1 The Coupling Schemes.....	199
4.2 The j -Coefficient Diagrams.....	201
4.3 Reduction of Diagrams.....	202
4.4 Examples.....	205
5. Multipole Operators.....	209
5.1 Integration over Electron Variables.....	209
5.2 The Angular Factor.....	210
6. Summarized Prescription.....	212
6.1 Step-by-Step Procedure.....	212
6.2 Example.....	214
7. Sums of Products of Matrix Elements.....	219
7.1 Effective Operators.....	219
7.2 Example.....	224
8. General Form of the Matrix Element.....	228
8.1 Graphical Representation.....	228
8.2 Evaluation of the Matrix Element.....	229

1. INTRODUCTION

In atomic and nuclear physics, many-particle wave functions are usually constructed as Slater determinants, i.e., as sums of products of one-particle wave functions. In a central-field approximation the one-particle functions are themselves products of radial, angular, and spin functions. The angular functions describe the symmetry of the wave functions under rotation and a many-particle wave function of a certain symmetry is obtained by coupling the one-particle angular wave functions in a specified way. In a sequence of papers, Racah (R42a, R42b, R43) developed calculational techniques for the evaluation of matrix elements of tensor operators between such many-particle wave functions. The original development concerned matrix elements which occur in theoretical atomic spectroscopy, but since then the methods have been used extensively in nuclear shell theory (deST63). In this

paper the discussion will be from the standpoint of atomic calculations.

Racah's guiding thought regarding spectroscopic calculations was that multiple integrations over angular coordinates reduce to standard, highly symmetric numerical functions of angular momentum quantum numbers, known today as $3n-j$ coefficients. This reduction has been performed over the years by a variety of techniques, utilizing points of view developed to unravel specific aspects of problems with increasing complication.

Today, sums of products of interaction matrix elements are carried out, or contemplated (RW63); these too can be reduced to a single operation (RS67, W68). The diagrammatic methods of Yutsis, Levinson, and Vanagas (YLV62), which can be combined with Feynman diagram techniques (J67), have been particularly effective in extending the range of application of Racah's concept. Several other points of view, mentioned below, have contributed to recent progress. It seems possible now to attempt a unified formulation which contains features from various sources and can be presented in a fairly self-contained manner.

A general approach of theoretical spectroscopy has been to utilize the analytical results of angular integrations without any attempt to evaluate radial integrals. Coefficients representing these integrals were determined by fitting large numbers of experimental energy levels. Thus the theory was used for the limited purpose of determining relationships among levels which are implied by angular momentum properties, i.e., by symmetries under rotation. Lately, interest has returned to radial integrations. This trend implies a shift in emphasis from a concentration on the effects of rotational symmetries to a more complete formulation which includes all relevant factors. It has been realized, of course, from the beginning that the effects of interaction of an atom with external, static or radiative, multipole fields could be treated on an equal footing with particle interactions within an atom (FR59, Chaps. 17-19). Nowadays, the methods of theoretical spectroscopy are normally applied to the collision phenomena; indeed, the relationship of the two fields is increasingly emphasized (FP63, Se66, SM68).

* Work performed under the auspices of the U.S. Atomic Energy Commission and supported by Contract No. C00-1674-37.

† Present address: Theoretical Physics Division, A.E.R.E., Harwell, Didcot, Berkshire, England.

Features of the theory which have been stressed by various authors and which will be combined in this paper include the following:

(1) Racah's basic formulas for the evaluation of the electrostatic interaction matrix elements concern a pair of electrons with given L and S . For multielectron systems, this interaction is evaluated by first recoupling each state of the matrix element so that the interacting electrons are paired together with given L and S . Basic formulas are then applied and the result is summed over all alternative values of L and S . Simplifications occurring in sums of this type suggest the existence of more flexible and convenient procedures. This consideration led Fano, Prats, and Goldschmidt (FPG63) to a procedure which reduces the angular integration in a matrix element between many-particle states to a single recoupling coefficient. The many- j coefficient can then be broken down into a product of simpler recoupling coefficients, or a sum of such products, in whichever way appears most expedient.

(2) Clebsch-Gordan (C-G) coefficients, recoupling coefficients, and the $3n-j$ coefficients can be represented graphically and algebraic operations with these quantities translated into graphical rules. The graphical representation of angular momentum coupling has found wide use, not only as a means of demonstrating symmetry properties (E57, FR59, J63), but in the actual performance of angular momentum calculations. The graphical method has the obvious advantage that it is easier to recognize relationships between pictorial representations of symmetric quantities than between the algebraic expressions themselves. The graphical representation of Yutsis, Levinson, and Vanagas (YLV62) has proved the most useful. The original formulation, based on a representation of the Wigner $3-j$ coefficient was subsequently extended to include C-G coefficients (YB65). Further developments, using the basic ideas of YLV62 were made by El-Baz and co-workers (MEL67, E69), who extended the graphical representation to include quantities, in addition to the $3-j$ coefficient, which appear frequently in the theory of angular momentum, for example, spherical harmonics, tensor operators, and elements of the rotation matrix. An important new feature was the graphical evaluation of reduced matrix elements of coupled tensor operators.

(3) In a product of interaction matrix elements such as occurs in the perturbation theory, a summation may be made over the states of the intermediate configurations of electrons. Since the one-electron states generated in the same central potential are orthogonal, each interaction operator in the product can be replaced by a "curtailed" operator. The matrix element of this operator is equal to that of the interaction operator when taken between the configurations in question and zero for all other configurations. The summation can then be extended over *all* states of the system since

intermediate configurations other than those in the initial product have zero matrix elements. A closure over the intermediate states allows the sequence of interaction matrix elements to be replaced by a single matrix element of an *effective* operator acting between the initial and final states only. The structure of this effective operator depends upon the intermediate configurations of particles. The replacement of perturbation terms by matrix elements of effective operators was first discussed by Bacher and Goudsmit (BG34). The first explicit calculations of the effective operators were by Rajnak and Wybourne (RW63). Racah and Stein (RS67) refined the calculations by introduction of the "curtailed" operators.

(4) In a second-quantization formalism the interaction operators are represented by Feynman graphs. Since the Feynman graphs are topologically equivalent to the angular momentum graphs of YLV62, these graphs automatically represent the angular momentum recoupling involved in the interaction. This equivalence between Feynman and angular momentum graphs has been utilized by Judd (J67) in analysing the tensor structure of the effective operators discussed in (3) above. Sandars (S69) made full use of the equivalence between Feynman and angular momentum diagrams to include all angular *and* radial factors in the graphical representation of a Coulomb interaction operator. Also, he showed specifically how to treat one-, two- and three-electron effective operators.

(5) The angular momentum recoupling involved in an interaction matrix element can be expressed, either algebraically or graphically, as a single recoupling coefficient. This recoupling coefficient is obtained from the procedure of FPG63 and is represented by a single graph. This procedure may be applied to the matrix element of any coupled tensor operator and also to sums of products of such matrix elements (Br70). Alternatively the graph may be obtained directly in two steps:

(a) bracketing the graph of the interaction operator by diagrams which represent the coupling of angular momenta in the many-particle states on the left- and right-hand sides of the matrix element (or product of matrix elements).

(b) combining the three graphs by joining all corresponding "open lines." This operation actually represents the integration or averaging over all orientation coordinates or magnetic quantum numbers. This fully diagrammatic procedure has been outlined by Matulis and Bandzaitis (MB65) and by Tolmachev (T69) but applied only to simple examples.

(6) Situations involving many electrons distributed in several open shells require an appropriate compact treatment of antisymmetrization for electrons in different shells and of the combined contribution of different equivalent electrons in any single shell. A standardized procedure introduced by Fano (F65) for

this purpose will be utilized in this paper. Consistent application of the creation operator algebra, using the commutation rules to take care of phase factors, leads to fully equivalent results as demonstrated by Armstrong (A68).

Bordarier (Bo70) has recently given a method for the evaluation of matrix elements which is based mainly on the graphical formulation of El-Baz (E69) and which overlaps considerably the method which will be given here. The scope of Bordarier's treatment is broad and encompasses many different types of matrix elements. It includes the graphical treatment of anti-symmetrization and fractional parentage. The cost of such generality is, of necessity, an increase in the number of graphical symbols. In this work the main objective will be more restricted, specifically the evaluation of matrix elements of Coulomb or one-electron tensor interaction operators (and products of such operators) between states with LS coupling. The point of view will be that of the user rather than the specialist. We will take advantage of the extreme simplification which is possible for this restricted class of examples in an attempt to give the easiest possible working procedure. Nevertheless, the method is capable of simple extension to the case of more complicated tensor operators and other schemes of coupling, as we will indicate in Sec. 8.

A recurring dilemma in the graphical method has been whether to use a representation based on the highly symmetric $3-j$ coefficients or on the C-G coefficients, which occur naturally in the calculation of matrix elements, but have lower symmetry. Attempts to resolve this question by the introduction of a graphical representation which can accommodate both coefficients simultaneously, notably by Brink and Satchler (BS68) and by El-Baz (E69), have resulted in a picture which is more coherent mathematically, but perhaps graphically less convenient. In this paper, again with a view to simplifying the working procedure, we find it expedient to use alternately both C-G and $3-j$ coefficients. In constructing a graphical representation of a matrix element, the simpler basis of C-G coefficients is more appropriate; in the reduction and evaluation of angular momentum graphs, where it is desirable to make use of symmetry properties, the basis of $3-j$ coefficients will be used.

The general rules of graphical calculation are contained in YLV62. Various workers have given selective summaries of these rules or the application of the rules to specific examples (BS69, E69, J67, S69, T69). In Sec. 4 of this paper a scheme will be developed for the systematic reduction of any angular momentum diagram to products (or sums of products) of $6-j$ coefficient diagrams. The $6-j$ coefficients are the only $3n-j$ coefficients which have received sufficiently extensive tabulation (RBMW59). The rules for graphical calculation are derived in this paper using

only the orthonormalization properties of C-G coefficients; it is assumed only that the reader is familiar with the properties of C-G coefficients, Wigner $3-j$ coefficients, and $6-j$ coefficients. The aim is to provide a self-contained procedure by which a complete numerical evaluation of the angular factor may be made, without recourse to tables of "standard" diagrams (YLV62) or to auxiliary computer programs. Nevertheless, the approach will be sufficiently flexible for it to be clear at which stage the individual user may take advantage of available alternative procedures to minimize the effort of calculation.

The development of techniques in this paper proceeds as follows. Section 2 describes the graphical representation firstly of the Coulomb interaction, secondly of the multipole interaction operators, and finally of the many-electron wave functions. In Sec. 3, the evaluation of matrix elements of the Coulomb operator is considered. The recoupling of angular momentum involved in each matrix element is obtained in the form of a single diagram. Section 4 gives the development of the graphical methods for the evaluation of this angular factor. In Sec. 5 the evaluation of matrix elements of a multipole interaction operator are considered. Section 6 summarizes the results of previous sections and gives a prescription which is illustrated by a worked example. In Sec. 7, sums of products of Coulomb and multipole interaction matrix elements are considered and in Sec. 8 some extensions of the method are discussed.

2. GRAPHICAL REPRESENTATION

In this section, interaction operators will be represented as sums of graphs which describe the interaction of particular sets of atomic subshells. The graphical representation is achieved by an expansion which separates the radial integrals and reduced matrix elements of tensor operators from other factors which are functions of magnetic quantum numbers.

Wave functions of atomic states will be also represented graphically. Integration over all electron coordinates will be performed symbolically by combining each interaction graph with the graphs of the atomic states involved in the matrix element. Each combined graph describes the recoupling of angular momenta involved in a single term of the final sum. Finally, rules will be derived for including relevant numerical factors, specifically a weight factor and a phase factor.

The graphical treatment parallels the algebraic evaluation of single matrix elements given by Fano (F65) and the notation of that paper will be used extensively.

2.1 The Interaction Operators

The states of one electron in a central field are specified in the usual notation of spectroscopy by the quantum numbers $nlm_s m_s$. The wave function of

electron i in the state $|nlmism_s\rangle$ will be written

$$(i | nlmism_s) = (r_i | nl) (\Omega_i | lm_i) (\Sigma_i | sm_s), \quad (2.1)$$

where r_i , Ω_i , Σ_i are the radial, angular, and spin coordinates, respectively, of electron i . The set of one-electron wave functions $(i | n_\lambda l_\lambda m_\lambda s_\lambda m_s)$ with alternative magnetic quantum numbers will be indicated by $(i | \lambda)$ for brevity.

The Coulomb interaction operator between electrons i and j is usually expanded in the form

$$V_{ij} = e^2 / |\mathbf{r}_i - \mathbf{r}_j| = e^2 \sum_k r_{<}^k / r_{>}^{k+1} P_k(\hat{\mathbf{r}}_i \cdot \hat{\mathbf{r}}_j). \quad (2.2)$$

Here $r_{>}$ and $r_{<}$ denote the greater and lesser of r_i , r_j , respectively, and P_k is a Legendre polynomial. P_k may be written as a scalar product of Racah tensors:

$$P_k(\hat{\mathbf{r}}_i \cdot \hat{\mathbf{r}}_j) = \mathbf{C}^{[k]}(\Omega_i) \cdot \mathbf{C}^{[k]}(\Omega_j) \\ = \sum_q (-1)^q C_q^{[k]}(\Omega_i) C_{-q}^{[k]}(\Omega_j), \quad (2.3)$$

where the components $C_q^{[k]}$ are spherical harmonics Y_{kq} normalized so that¹

$$\sum_q |C_q^{[k]}|^2 = 1,$$

i.e.,

$$C_q^{[k]} = [4\pi / (2k+1)]^{1/2} Y_{kq}.$$

The tensor components $C_q^{[k]}$ in Eq. (2.3) may be separately expanded by making use of the Wigner-Eckart theorem, i.e.,

$$C_q^{[k]}(\Omega_i) = \sum_{lm} \sum_{l'm'} (\Omega_i | lm) (lm | C_q^{[k]} | l'm') (l'm' | \Omega_i) \\ = \sum_{lm} \sum_{l'm'} [l]^{-1/2} (lm | l'm'kq) (\Omega_i | lm) \\ \times (l || C^{[k]} || l') (l'm' | \Omega_i), \quad (2.4)$$

where a factor $(-1)^{2k}$ has been canceled since k is integral. Here the sums over m, m' are no longer independent but are subject to the restriction $m' + q = m$. Also, here and throughout, we make the now customary abbreviation $[l] \equiv 2l+1$.

By applying the transformation (2.4) to both com-

¹ We will use the normalization convention which has $Y_{k0} = (2k+1/4\pi)^{1/2} P_k(\cos\theta)$. This gives the following formula for the reduced matrix element of $C^{[k]}$,

$$(l || C^{[k]} || l') = (-1)^l ([l][l'])^{1/2} \begin{pmatrix} l & k & l' \\ 0 & 0 & 0 \end{pmatrix}.$$

This is the normalization convention of R42b and CS35. The Y_{kq} defined by Fano and Racah (FR59) contain an additional factor i^k . The phase convention of FR59 is used in F65, RS67, and A68. Consequently the $(l || C^{[k]} || l')$ given by Eq. (14.12) of FR59 should be used in the results of these papers. Also, it must be emphasized that the *atomic states* of FR59 differ in phase from those commonly used (which are those used in this paper) since the angular part $(\Omega | lm)$ of the one-electron wave functions of FR59 contain the additional factor i^l . This phase difference must be recognized when making comparison between matrix elements involving many-electron wave functions defined according to the two phase conventions.

ponents of the Racah tensor on the right-hand side of Eq. (2.3), substituting the resulting expression in Eq. (2.2), extending the summation over *all* quantum numbers, and performing the radial integration, we obtain the result

$$V_{ij} = \sum_k \sum_{\lambda\mu} \sum_{\lambda'\mu'} R^k(n_\lambda l_\lambda n_\mu l_\mu, n_{\lambda'} l_{\lambda'} n_{\mu'} l_{\mu'}) (l_\lambda || C^{[k]} || l_{\lambda'}) \\ \times (l_\mu || C^{[k]} || l_{\mu'}) [(i | \lambda) (j | \mu) \{\lambda' | i\} \{\mu' | j\}] \\ \times \sum_q (-1)^q [l_\lambda]^{-1/2} [l_\mu]^{-1/2} \\ \times (l_\lambda m_\lambda | l_{\lambda'} m_{\lambda'} k q) (l_\mu m_\mu | l_{\mu'} m_{\mu'} k - q), \quad (2.5)$$

where $R^k(n_\lambda l_\lambda n_\mu l_\mu, n_{\lambda'} l_{\lambda'} n_{\mu'} l_{\mu'})$ is the Slater radial integral defined by Condon and Shortley (CS35). Henceforth we will use an abbreviation introduced by Rajnak and Wybourne (RW63), viz.,

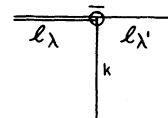
$$X(k; \lambda\mu\lambda'\mu') \equiv R^k(n_\lambda l_\lambda n_\mu l_\mu, n_{\lambda'} l_{\lambda'} n_{\mu'} l_{\mu'}) \\ \times (l_\lambda || C^{[k]} || l_{\lambda'}) (l_\mu || C^{[k]} || l_{\mu'}). \quad (2.6)$$

Using the transformation properties of C-G coefficients we can write Eq. (2.5) in the form

$$V_{ij} = \sum_k \sum_{\lambda\mu} \sum_{\lambda'\mu'} X(k; \lambda\mu\lambda'\mu') \\ \times [(i | \lambda) (j | \mu) \{\lambda' | i\} \{\mu' | j\}] (-1)^k \sum_q [l_\lambda]^{-1/2} \\ \times [l_{\mu'}]^{-1/2} (l_\lambda m_\lambda | l_{\lambda'} m_{\lambda'} k q) (l_{\mu'} m_{\mu'} | l_\mu m_\mu k q), \quad (2.7)$$

where we have also used the fact that $l_\mu + k - l_{\mu'}$ is even. This follows since $l_{\mu'}$ is integral and the factor $(l_\mu || C^{[k]} || l_{\mu'})$ vanishes unless $(l_\mu + k + l_{\mu'})$ is an even integer.

Each C-G coefficient on the right-hand side of Eq. (2.7) will be represented graphically by a vertex at which three lines meet. Each line is labeled with one of the momenta involved in the C-G coefficient. The coupling scheme amongst the three momenta is indicated by a sign on the vertex (or node, as it will be called) and by drawing a thick line to distinguish the resultant from the compounded momenta. If the sequence of angular momenta $(j_1 j_2) j$ in the C-G coefficient $(j_1 m_1 j_2 m_2 | j m)$ is obtained by reading the lines in clockwise order about the node, the node carries a minus sign. If the sequence is reproduced by reading the lines in anticlockwise order, the node carries a plus sign. This is the convention adopted by Yutsis and Bandzaitis (YB65). For example, the coefficient $(l_\lambda m_\lambda | l_{\lambda'} m_{\lambda'} k q)$ has the following graphical representation:



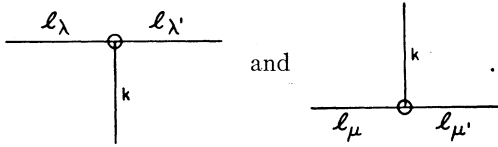
When divided by the factor $[l_\lambda]^{1/2}$, the C-G coeffi-

cient $(l_\lambda m_\lambda | l_{\lambda'} m_{\lambda'} k q)$ equals, to within a phase factor, the 3- j coefficient

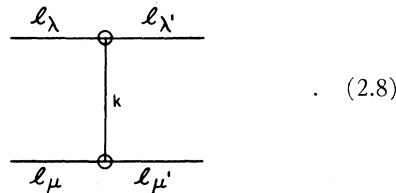
$$\begin{pmatrix} l_{\lambda'} & k & l_\lambda \\ m_{\lambda'} & q & -m_\lambda \end{pmatrix}$$

in which the three momenta appear on an equal footing. For this reason, the factor $[l_\lambda]^{-1/2} (l_\lambda m_\lambda | l_{\lambda'} m_{\lambda'} k q)$ will be represented by a graph in which the three lines are of equal thickness. Further, from the transformation properties of the C-G coefficient, a change in the orientation of the node (i.e., in the sign) is equivalent to multiplying by a factor $(-1)^{l_{\lambda'}+k-l_\lambda}$, which is positive in this case as discussed above. This means that the sign on the node becomes redundant in the representation of the C-G coefficients on the right-hand side of Eq. (2.7). Therefore the signs will be omitted.

The two C-G coefficients on the right-hand side of (2.7), multiplied by the factors $[l_\lambda]^{-1/2}$ and $[l_\mu]^{-1/2}$, will be represented by the following graphs:



The summation over q is achieved symbolically by joining the two free k lines to give the graph



In this graph the k line is closed, i.e., both ends terminate in nodes, corresponding to the fact that the algebraic expression it represents is not a function of q after summation.

The graph (2.8) represents only the coupling of orbital angular momenta in the sum over products of C-G coefficients in Eq. (2.5) and so may be deformed in any way so long as the nodes represent the triads of momenta $(l_\lambda k l_{\lambda'})$ and $(l_\mu k l_{\mu'})$. The graph has been drawn with the λ, μ lines open to the left and the λ', μ' lines open to the right so that its meaning may be extended to include all factors on the right-hand side of Eq. (2.5). Accordingly, the interaction operator V_{ij}

will be written

$$V_{ij} = \sum_{\lambda\lambda'} \sum_{\mu\mu'} \sum_k \begin{array}{c} \lambda \quad \lambda' \\ \text{---} \circ \text{---} \\ | \\ \text{---} \times \text{---} \\ | \\ \mu \quad \mu' \\ \text{---} \circ \text{---} \end{array} \quad (2.9)$$

Here the labels $\lambda, \lambda', \mu, \mu'$ denote all one-electron quantum numbers. The line labeled λ , with the left-hand end free and labeled i , represents the one-electron wave function $(i | n_\lambda l_\lambda m_i s_\lambda m_s)$. Similarly the line labeled μ' with the right-hand end free and labeled j represents the one-electron wave function $(n_{\mu'} l_{\mu'} m_{i'} s_{\mu'} m_{s'} | j)$, etc. Also, the cross on the closed line represents the factor $(-1)^k X(k; \lambda \mu \lambda' \mu')$.

The same principles can be applied to the multipole moment operator $\sum_i r_i^k C_q^{[k]}(\Omega_i)$. Use of the transformation (2.4) gives the result

$$r_i^k C_q^{[k]}(\Omega_i) = \sum_{\lambda\lambda'} I(k; \lambda\lambda') [(i | \lambda \rangle \langle \lambda' | i)] \times [l_\lambda]^{-1/2} (l_\lambda m_\lambda | l_{\lambda'} m_{\lambda'} k q), \quad (2.10)$$

where we define

$$I(k; \lambda\lambda') \equiv (n_\lambda l_\lambda | r^k | n_{\lambda'} l_{\lambda'}) (l_\lambda || C^{[k]} || l_{\lambda'}). \quad (2.11)$$

The right-hand side of Eq. (2.10) can similarly be represented graphically to give

$$r_i^k C_q^{[k]}(\Omega_i) = \sum_{\lambda\lambda'} \begin{array}{c} | \\ | \\ | \\ \text{---} \text{---} \text{---} \\ | \\ \lambda \quad \lambda' \end{array} \quad (2.12)$$

In this case, the double bar on the k line represents a factor $I(k; \lambda\lambda')$ and the label q on the k line denotes the component q of the tensor operator.²

2.2 Many-Electron Wavefunctions

Different configurations of atomic electrons will be denoted by the letters A, B, C , etc. These configurations are specified by the number of equivalent electrons occupying each atomic subshell. In accord with our previous notation, the successive atomic subshells $1s, 2s, 2p$, etc., will be denoted by successive values of the index λ .

Fano (F65) has given a detailed discussion of the construction of a fully antisymmetric wave function for a state of a configuration A of N electrons having N_λ electrons in the λ th subshell. In an LS scheme of

² Clearly, any tensor operator of the form $\sum_i f(k, r_i) C_q^{[k]}(\Omega_i)$ can be represented by a form like the right-hand side of (2.12).

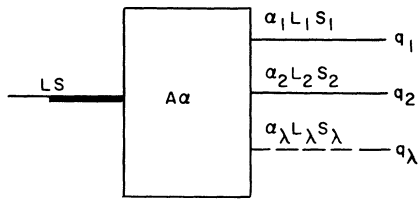
coupling (which we will use throughout), the N_λ electrons of subshell λ are coupled to total subshell quantum numbers $\alpha_\lambda L_\lambda S_\lambda M_{L,\lambda} M_{S,\lambda}$, where α_λ denotes all other quantum numbers (e.g., seniority) necessary to specify the state uniquely. The one-electron variables $r_i \Omega_i \Sigma_i$ of the N_λ electrons of subshell λ will be prescribed to be ordered in the sequence of *increasing* i . The ordered set of such variables will be indicated by q_λ . An antisymmetrized wave function of subshell λ will be indicated by $(n_\lambda l_\lambda^{N_\lambda} \alpha_\lambda L_\lambda S_\lambda M_{L,\lambda} M_{S,\lambda} | q_\lambda)$ and the set of such wave functions with alternative M quantum numbers by

$$\{n_\lambda l_\lambda^{N_\lambda} \alpha_\lambda L_\lambda S_\lambda | q_\lambda\}. \quad (2.13)$$

An *unsymmetrized* wave function of the N electrons is constructed by multiplying together all subshell wave functions (2.13) and coupling their angular momenta according to some scheme, denoted by α , to give resultant L and S total quantum numbers, i.e.,

$$(A\alpha LSM_L M_S | q) \\ = [\prod_\lambda \{n_\lambda l_\lambda^{N_\lambda} \alpha_\lambda L_\lambda S_\lambda | q_\lambda\}]_{M_L M_S}^{(\alpha L S)}.$$

Here A denotes the configuration and q denotes the aggregate $\{q_\lambda\}$ of ordered sets of subshell variables. Such a wave function will be represented graphically by drawing a single line to represent each subshell wave function and joining the lines according to the prescription denoted by α . The scheme α can remain unspecified for the moment so that the set of unsymmetrized atomic wave functions with alternative M_L, M_S quantum numbers will be represented by



$$(2.14)$$

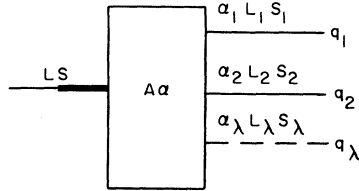
For the purpose of subsequently establishing a standardized phase convention, the subshells are ordered vertically downwards in the direction of increasing λ .

The index q specifies the distribution of electrons amongst the subshells. Each distribution is assigned a parity P_q according to the number of permutations by which it differs from the standard order 1, 2... N of the electrons, i.e., from the distribution with electrons 1, 2 in the 1s subshell, electrons 3, 4 in the 2s subshell, etc. The number of distinct distributions of the N

electrons amongst the subshells is

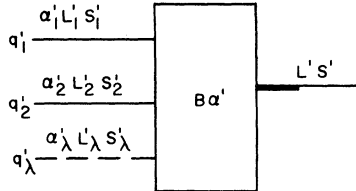
$$\mathfrak{N} = N! / (\prod_\lambda N_\lambda!).$$

The set of normalized N -electron *antisymmetrized* wave functions with different M quantum numbers is obtained by summing (2.14) over all distributions q , i.e.,



$$\mathfrak{N}^{-1/2} \sum_q (-1)^{P_q} \quad (2.15)$$

Similarly, the wave functions of the N -electron state $|B\alpha' L' S'\rangle$, having N_λ' electrons in the λ th subshell will be written



$$\mathfrak{N}'^{-1/2} \sum_{q'} (-1)^{P_{q'}} \quad (2.16)$$

2.3 Fractional Parentage Expansion

In the evaluation of matrix elements it is necessary to separate one or more electrons from the subshell of N_λ equivalent electrons such that they are coupled onto, but no longer antisymmetrized with, the remaining electrons. This is achieved by a fractional parentage (f.p.) expansion, which for one electron is

$$\{n_\lambda l_\lambda^{N_\lambda} \alpha_\lambda L_\lambda S_\lambda | q_\lambda\} \\ = \sum_{\text{f.p.}} (l_\lambda^{N_\lambda} \alpha_\lambda L_\lambda S_\lambda | l_\lambda^{N_\lambda-1} \bar{\alpha}_\lambda \bar{L}_\lambda \bar{S}_\lambda, l_\lambda) \\ \times [\{n_\lambda l_\lambda^{N_\lambda-1} \bar{\alpha}_\lambda \bar{L}_\lambda \bar{S}_\lambda | \bar{q}_\lambda\} \times \{ \lambda | i \}]^{(L_\lambda S_\lambda)}. \quad (2.17)$$

Here and throughout, a summation sign labeled "f.p." will be used to denote a summation over fractional

parentage. In all cases, the quantum numbers to be summed over will be those which carry a bar or a tilde, e.g., $\bar{\alpha}_\lambda \bar{L}_\lambda \bar{S}_\lambda$ or $\tilde{\alpha}_\lambda \tilde{L}_\lambda \tilde{S}_\lambda$. Here i is the largest of the indices in the set q_λ , and \bar{q}_λ denotes the set which remains after the removal of i . The fractional parentage expansion will be represented graphically by making the substitution

$$\begin{aligned}
 & \text{---} \circ \text{---} \alpha_\lambda L_\lambda S_\lambda \text{---} q_\lambda \\
 = & \sum_{\text{f.p.}} \left[\text{---} \circ \text{---} \alpha_\lambda L_\lambda S_\lambda \text{---} \blacksquare \text{---} \bar{\alpha}_\lambda \bar{L}_\lambda \bar{S}_\lambda \text{---} \bar{q}_\lambda \right. \\
 & \quad \left. \begin{array}{l} \diagdown \lambda \\ \diagdown i \end{array} \right] \quad (2.18)
 \end{aligned}$$

in the diagrams like (2.15). The full square on the node represents the coefficient of fractional parentage (c.f.p.) $(l_\lambda^{N\lambda} \alpha_\lambda L_\lambda S_\lambda \{ | l_\lambda^{N\lambda-1} \bar{\alpha}_\lambda \bar{L}_\lambda \bar{S}_\lambda, l_\lambda \})$ in (2.17). The diagram on the right hand side of (2.18) represents the C-G coefficient describing the coupling of momenta on the right hand side of (2.17). In a similar way, when two electrons are separated out of the same subshell, we use the two-electron coefficient of fractional parentage defined by Racah (R43) and make the substitution

$$\begin{aligned}
 & \text{---} \circ \text{---} \alpha_\lambda L_\lambda S_\lambda \text{---} q_\lambda \\
 = & \sum_{\text{f.p.}} \left[\text{---} \circ \text{---} \alpha_\lambda L_\lambda S_\lambda \text{---} \blacksquare \text{---} \bar{\alpha}_\lambda \bar{L}_\lambda \bar{S}_\lambda \text{---} \bar{q}_\lambda \right. \\
 & \quad \left. \begin{array}{l} \diagdown \tilde{\lambda} \tilde{S}_\lambda \\ \diagdown \lambda \\ \diagdown i \end{array} \right] \quad (2.19)
 \end{aligned}$$

where the full square represents the two-electron c.f.p. $(l_\lambda^{N\lambda} \alpha_\lambda L_\lambda S_\lambda \{ | l_\lambda^{N\lambda-2} \bar{\alpha}_\lambda \bar{L}_\lambda \bar{S}_\lambda, l_\lambda^2 \tilde{L}_\lambda \tilde{S}_\lambda \})$ and i and j are the largest and next-largest values of the indices in the set q_λ .

3. THE COULOMB MATRIX ELEMENT

We will consider the matrix element of the Coulomb interaction between the states $(A, \alpha LS |$ and $| B, \alpha' L' S' \rangle$, i.e.,

$$M = (A, \alpha LS | \sum_{i < j}^N V_{ij} | B, \alpha' L' S' \rangle. \quad (3.1)$$

The Coulomb matrix element is diagonal in the total magnetic quantum numbers $M_L M_S$ which have been suppressed in (3.1) for brevity.

3.1 Integration over Electron Variables

Since each term V_{ij} contributes equally to the matrix element (3.1) we have

$$M = \frac{1}{2} N(N-1) (A, \alpha LS | V_{N-1, N} | B, \alpha' L' S' \rangle. \quad (3.2)$$

This form of the matrix element singles out electrons $N-1, N$ as interacting electrons while the rest remain "spectators."

The evaluation of the matrix element proceeds by bracketing the representation (2.9) of the Coulomb operator $V_{N-1, N}$ by the representations (2.15) and (2.16) of the atomic wave functions. The interacting electrons $N-1, N$ are distinguished from other equivalent electrons by fractional parentage expansions, such as (2.18), of the relevant subshell wave functions. Integration over electron coordinates *and* summation over magnetic substates is achieved symbolically by joining free lines corresponding to the same electron or group of electrons. This graphical operation will be called "contraction."

The orthogonality of one-electron wave functions means that the joining of free lines gives a nonzero result only when the lines represent the same electron or group of electrons and carry the same quantum number labels. This property results in a drastic reduction in the number and kind of terms contributing to M in the following two ways:

(1) The summation over $\lambda \mu \lambda' \mu'$ in the operator representation (2.9) is restricted to a small number of terms. The operator changes the quantum numbers of only two electrons so that M vanishes if the configurations A and B differ in the quantum numbers of more than two electrons. If the configurations differ in the quantum numbers of just two electrons, then there are contributions from a single set of interacting subshells $\{ \lambda \mu, \lambda' \mu' \}$. Otherwise there are alternative choices of the set $\{ \lambda \mu, \lambda' \mu' \}$. However, the contribution to M of each term in the summation, which we will call $M(\lambda \mu \lambda' \mu')$, may be evaluated *independently*. This means that the summation over $\lambda \mu \lambda' \mu'$ may be brought outside the matrix element, i.e., we put

$$M = \sum_{\lambda \mu \lambda' \mu'} M(\lambda \mu \lambda' \mu'). \quad (3.3)$$

Henceforth we shall consider the contribution of one particular term in the sum (3.3), say $M(\rho \sigma \rho' \sigma')$, and assume that $\rho < \sigma, \rho' < \sigma'$.

(2) The summations over qq' in (2.15) and (2.16) are restricted to those terms which are diagonal in the distributions $\bar{q} = \{ \bar{q}_\lambda \}$ and $\bar{q}' = \{ \bar{q}'_{\lambda'} \}$ of spectator electrons among the subshells. Again this follows from the fact that the interaction operator changes only the quantum numbers of *interacting* electrons. Each diagonal term contributes equally so that we need consider specifically only one such distribution \bar{q} and multiply

by the number

$$\bar{\mathfrak{N}} = (N-2)! / (\prod_{\lambda} \bar{N}_{\lambda}!) \quad (3.4)$$

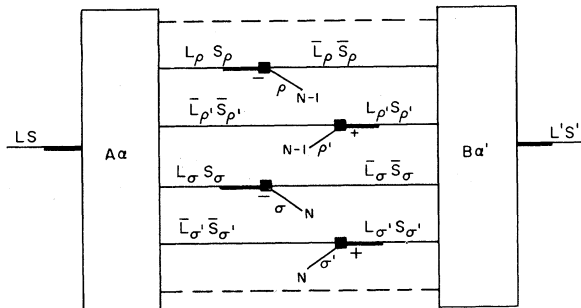
of such distributions.

There now remains only the permutation of the interacting electrons. The term $M(\rho\sigma\rho'\sigma')$ is the matrix element of the operator

$$\sum_k \begin{array}{c} \rho \quad \rho' \\ \text{---} \text{---} \\ \text{---} \text{---} \\ \text{---} \text{---} \\ \text{---} \text{---} \\ \sigma \quad \sigma' \end{array} \quad (3.5)$$

in the sum (2.9) for $V_{N-1,N}$. Therefore, the distribution of interacting electrons is fixed, with electrons $N-1, N$ in the ρ, σ subshells in the left-hand wave function and the ρ', σ' subshells in the right-hand wave function respectively.

The distributions q, q' are now fixed. After separation of the interacting electrons by f.p. expansions of the type (2.18), the integration over spectator electrons is achieved by contracting corresponding free lines in the terms with the required electron distribution in (2.15) and (2.16). The graph resulting from this contraction is of the form

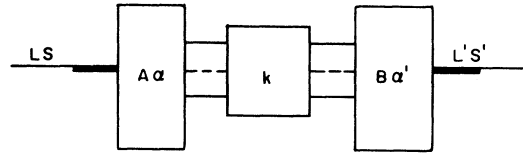


(3.6)

The remaining integration over the coordinates of the spectator electrons is performed by contracting the operator graph (3.5) with graph (3.6). This contraction completes the integration. From (3.2), (2.15), (2.16), and (3.4) the term $M(\rho\sigma\rho'\sigma')$ has been obtained in

the form,

$$M(\rho\sigma\rho'\sigma') = [\frac{1}{2}N(N-1)\bar{\mathfrak{N}}^{-1/2}\bar{\mathfrak{N}}'^{-1/2}\bar{\mathfrak{N}}](-1)^{P_q+P_{q'}} \sum_k \sum_{f.p.}$$



(3.7)

The phase factors in this expression will be given explicitly in Sec. 3.2. The central block in the diagram in (3.7) represents the coupling of the interacting electron lines with the k line. The diagram is multiplied by the factor $(-1)^k X(k; \rho\sigma\rho'\sigma')$ and the cross on the k line is erased. Similarly the full squares on the nodes involved in the f.p. expansions are erased by multiplying the diagram by the appropriate c.f.p. The diagram now is a function of angular momentum quantum numbers only, since the *radial* integration contributes to the factor $X(k; \rho\sigma\rho'\sigma')$, which has been removed from the diagram. The evaluation of the numerical function which the angular diagram represents will be given in Sec. 4.

For a given set of subshells $\{\rho\sigma, \rho'\sigma'\}$ there are other terms contributing to the sum (3.3). These must be added to $M(\rho\sigma\rho'\sigma')$. Then the sum of contributions from all other sets of interacting subshells are added to complete the evaluation of the Coulomb matrix element M as indicated by Eq. (3.3).

3.2 Phase Factor and Weight Factor

The phase factors and weight factors can be conveniently separated into two contributions. First, there is a contribution from the summation over different distributions $\{\bar{q}_{\lambda}\}$ of the spectator electrons. Second, there is a contribution from different ordering of the interacting electrons themselves. The former depends upon the subshell occupation numbers only and will be considered first.

The relevant weight factors have been given in (3.7). Where the interacting electrons occupy subshells ρ, σ on the left and ρ', σ' on the right, we find

$$\frac{1}{2}N(N-1)\bar{\mathfrak{N}}(\bar{\mathfrak{N}}\bar{\mathfrak{N}}')^{-1/2} = \frac{1}{2}[N_{\rho}(N_{\sigma}-\delta_{\rho\sigma})N_{\rho'}(N_{\sigma'}-\delta_{\rho'\sigma'})]^{1/2} \quad (3.8)$$

by using (3.4). Aside from the factor $\frac{1}{2}$, this weight factor is the square root of the product of the number of electrons which can be drawn from each of the relevant interacting subshells.

There is a phase factor $(-1)^{P_q+P_{q'}}$ associated with

the distributions of the electrons in left-hand and right-hand wave functions. Since the parity $P_{\bar{q}}$ of the distribution of spectator electrons is the same in both wave functions, we need consider only the parity of the permutation which shifts the *interacting* electrons from their "natural" order $N-1, N$ (see Sec. 2.2). The permutation which shifts the pair of interacting electrons into the appropriate subshells *without regard to the order of the interacting electrons themselves* has parity

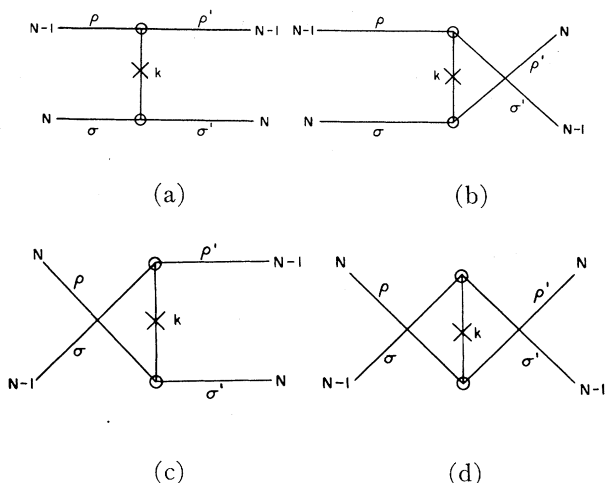
$$P_A = \sum_{\lambda=\rho+1}^{\infty} \bar{N}_{\lambda} + \sum_{\lambda=\sigma+1}^{\infty} \bar{N}_{\lambda} \quad (3.9)$$

for the left-hand state and

$$P_B = \sum_{\lambda=\rho'+1}^{\infty} \bar{N}_{\lambda} + \sum_{\lambda=\sigma'+1}^{\infty} \bar{N}_{\lambda} \quad (3.10)$$

for the right-hand state. This expression can be simplified because only the difference $P_A - P_B$ is relevant at this point. However, we postpone the simplification because the generality of (3.9) and (3.10) will be of use in Sec. 6. Phase factors such as (3.9) and (3.10) which come from the antisymmetrization of the many-electron wave functions will be called "Pauli phase factors."

The factors (3.8)–(3.10) depend only upon *which* subshells are involved in the interaction, and so are the same for all terms $M(\lambda\mu\lambda'\mu')$ contributing to the interaction among the set $\{\lambda\mu, \lambda'\mu'\}$. In Sec. 3.1 we considered the particular term $M(\rho\sigma\rho'\sigma')$. We now consider the other terms in (3.3) arising from the same choice of subshells. The set of subshells $\{\rho\sigma, \rho'\sigma'\}$ contributes four terms, $M(\rho\sigma\rho'\sigma')$, $M(\rho\sigma\sigma'\rho')$, $M(\sigma\rho\rho'\sigma')$, and $M(\sigma\rho\sigma'\rho')$, to the matrix element M . These terms arise from the following four terms of the sum (2.9) for the operator $V_{N-1, N}$,



(3.11)

In drawing the graphs (3.11) we have assumed that

$\rho < \sigma$ and $\rho' < \sigma'$, and followed the convention that subshells are ordered vertically downwards.

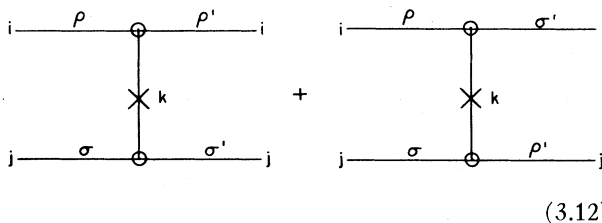
In (a), the electrons are in standard order on both sides of the interaction graph so that by convention we associate a phase +1 with this graph. The graphs (b) and (c) have a single permutation of the electrons and so contribute a phase factor (-1). The graph (d) has the electrons interchanged on both sides and so has a phase +1.

Clearly, when the graphs are drawn with subshells ordered vertically downwards, a permutation of the electrons between subshells results in a crossing of one-electron lines. This leads to the simple rule that a phase factor -1 is included for each time that one-electron lines cross.

We now take advantage of the fact that permutation of electrons $N-1$ and N on *both* sides of the matrix element has no net effect. Graph (a) includes the factor $X(k; \rho\sigma\rho'\sigma')$ and graph (d) includes the factor $X(k; \sigma\rho\rho'\sigma')$. These factors coincide on account of the symmetry of the Slater radial integral in (2.6). Similarly, graphs (b) and (c) include the factors $X(k; \rho\sigma\sigma'\rho')$ and $X(k; \sigma\rho\rho'\sigma')$ respectively, which are equal. Furthermore, since the orientation of the nodes involving a k line is not significant, graphs (a) and (d) give the same result upon contraction with the appropriate graphs like (3.6). [The ordering convention fixes the relative vertical positions of the free lines and so graph (d) can be made coincident with graph (a) by rotating the k line of graph (d) through 180° about a horizontal axis in the plane of the paper.] By the same argument, graphs (b) and (c) also lead to equivalent diagrams. This means that we need consider only the graphs which are distinct in the *pairs* of subshells coupled by the k line.

Each distinct graph then has a weight factor 2 which cancels the factor $\frac{1}{2}$ in (3.7). Accordingly, for the case $\rho \neq \sigma, \rho' \neq \sigma'$, the part of the Coulomb interaction attributable to interaction among the subshells $\rho\sigma\rho'\sigma'$ is obtained by taking the matrix element of the operator $\bar{V}(\rho\sigma, \rho'\sigma')$

$$= \sum_{i \neq j} \bar{V}_{ij}(\rho\sigma, \rho'\sigma') = \sum_{i \neq j} \sum_k$$



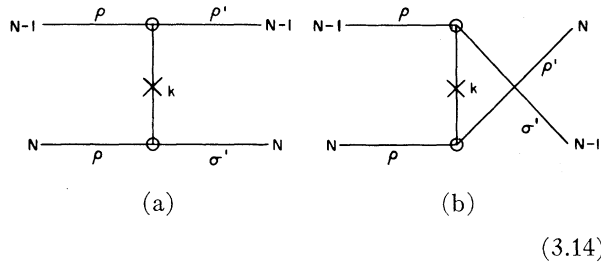
(3.12)

between the states $(A\alpha |$ and $| B\alpha')$. The form (3.12) is equivalent to the "curtailed" operators used by Racah and Stein (RS67). As in that paper, we will use this form in the discussion of products of matrix elements in Sec. 7.

The matrix element of the curtailed operator (3.12) between the states $(A\alpha |$ and $| B\alpha')$ gives the sum of the contributions to the full Coulomb matrix element of the terms involving the set of subshells $\{\rho\sigma, \rho'\sigma'\}$. Indicating the matrix element of the curtailed operator by $\bar{M}(\rho\sigma, \rho'\sigma')$, we have

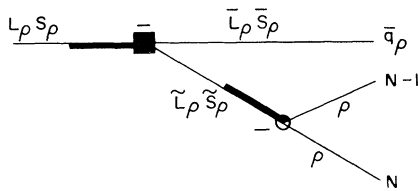
$$\bar{M}(\rho\sigma, \rho'\sigma') = M(\rho\sigma\rho'\sigma') + M(\rho\sigma\sigma'\rho') + M(\sigma\rho\rho'\sigma') + M(\sigma\rho\sigma'\rho'). \quad (3.13)$$

The case where two electrons are transferred out of the same subshell in one state only is typified by the situation $\rho=\sigma, \rho'\neq\sigma'$. Here, there are just two contributions to the interaction operator $V_{N-1,N}$, viz.,



(3.14)

The graph (b) has a phase (-1) with respect to graph (a) and at first sight the graphs appear distinct. However, the graphs include coincident factors $X(k; \rho\rho\rho'\sigma')$ and $X(k; \rho\rho\sigma'\rho')$. Also, both graphs are contracted with graphs like (3.6) in which the interacting electrons have been separated from the ρ subshell by a two-electron f.p. expansion (2.19). The terms of the f.p. expansion are represented by graphs,

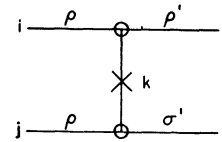


(3.15)

When the graph (b) of (3.14) is contracted with graph (3.15) and the positions of the two ρ lines are then interchanged, the result is identical to the contraction of (a) with (3.15). Interchanging the two ρ lines corresponds to changing the coupling $(l_{\rho, N-1} l_{\rho, N}) \bar{L}_{\rho} \bar{S}_{\rho}$ to the coupling $(l_{\rho, N} l_{\rho, N-1}) \bar{L}_{\rho} \bar{S}_{\rho}$. This change introduces a factor $(-1)^{-\bar{L}_{\rho} - \bar{S}_{\rho} + 2l_{\rho} + 1}$, where both electrons have spin $\frac{1}{2}$. The orbital momentum l_{ρ} is integral and $(\bar{L}_{\rho} + \bar{S}_{\rho})$ is even for a pair of equivalent electrons, so that the interchange of ρ lines introduces a

factor -1 . Therefore the contributions of graphs (a) and (b) to the matrix element are equal. Again, only graph (a) need be considered, with a weight factor 2, which cancels the factor $\frac{1}{2}$ in (3.8). For the contribution of the set of subshells $\{\rho\rho, \rho'\sigma'\}$ to the Coulomb interaction we will use the operator

$$\bar{V}(\rho\rho, \rho'\sigma') = \sum_{i \neq j} \bar{V}_{ij}(\rho\rho, \rho'\sigma') = \sum_{i \neq j} \sum_k$$



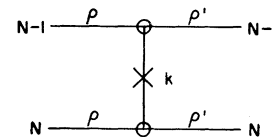
(3.16)

in Sec. 7.

Denoting the matrix element of the curtailed operator (3.16) between $(A\alpha |$ and $| B\alpha')$ by $\bar{M}(\rho\rho, \rho'\sigma')$, we have

$$\bar{M}(\rho\rho, \rho'\sigma') = M(\rho\rho\rho'\sigma') + M(\rho\rho\sigma'\rho'). \quad (3.17)$$

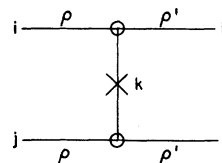
Finally, in the case where $\rho=\sigma$ and $\rho'=\sigma'$, there is only one term which contributes to the operator $V_{N-1,N}$, viz.,



(3.18)

and the factor $\frac{1}{2}$ is not canceled from (3.8). In this case the contribution of the interaction between the subshells ρ and ρ' is given by the matrix element of the operator

$$\bar{V}(\rho\rho, \rho'\rho') = \sum_{i < j} \bar{V}_{ij}(\rho\rho, \rho'\rho') = \sum_{i < j} \sum_k$$



(3.19)

where the $i < j$ condition replaces the factor $\frac{1}{2}$ in (3.8).

Trivially, in this case we have

$$\bar{M}(\rho\rho, \rho'\rho') = M(\rho\rho\rho'\rho'). \quad (3.20)$$

It has been demonstrated that the contribution of a particular set of subshells to the Coulomb interaction between states of the configuration A and B is equal to the matrix element of a curtailed operator between the same states. The graphical representation of the curtailed operators (3.12), (3.16), or (3.19) contain only those graphs which are distinct in the *pairs* of subshells which are coupled by the interaction. The full Coulomb matrix element M is then equal to the sum of the matrix elements of the curtailed operators corresponding to each set of subshells which contributes to the Coulomb interaction. From (3.13), (3.17), and (3.20) we see that the sum M in (3.3) may be replaced by

$$M = \sum_{\{\lambda\mu, \lambda'\mu'\}} \bar{M}(\lambda\mu, \lambda'\mu'), \quad (3.21)$$

where the summation is now over the distinct *sets* of subshells which give a nonzero contribution.

4. EVALUATION OF THE ANGULAR FACTOR

After removal of the cross on the k line [denoting the factor $(-1)^k X(k; \lambda\mu\lambda'\mu')$] and the full squares on certain nodes (denoting the c.f.p.), the diagram on the right-hand side of (3.7) is a function of k and the angular momentum quantum numbers only. The labels λ , etc., on one-electron lines can now be replaced by the corresponding angular quantum numbers $l_{\lambda s_{\lambda}}$, etc. Also, other quantum numbers denoted by α_{λ} , etc., can be removed from the diagram. We will call this diagram the “ \mathcal{g} diagram,” or simply “ \mathcal{g} .”

The \mathcal{g} diagram may be regarded as the inner product of two wave functions of the same basic angular momenta coupled by different schemes of addition, i.e., as a coefficient of the form

$$((j_1 j_2 \dots j_n) \alpha JM | (j_1 j_2 \dots j_n) \alpha' JM), \quad (4.1)$$

where α, α' denote the coupling schemes. In the coefficient represented by the diagram on the right-hand side of (3.7), the coupled momenta $j_1 j_2 \dots j_n$ are the momentum k , the interacting electron momenta $l_{\lambda s_{\lambda}}$, etc., and the momenta $\bar{L}_{\lambda} \bar{S}_{\lambda}$, etc., of groups of spectator electrons.

The coefficient (4.1) is independent of M and so is equal to its average over all magnetic substates, i.e.,

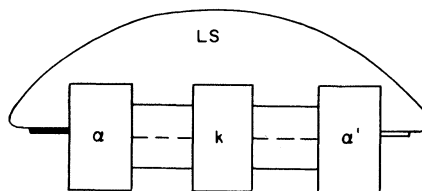
$$\begin{aligned} & ((j_1 j_2 \dots j_n) \alpha J | (j_1 j_2 \dots j_n) \alpha' J) \\ &= [J]^{-1} \sum_M ((j_1 j_2 \dots j_n) \alpha JM | (j_1 j_2 \dots j_n) \alpha' JM). \end{aligned} \quad (4.2)$$

The coefficient on the left-hand side of (4.2) is a *re-coupling coefficient* (FR59), also called a *transformation matrix* (YLV62). The numerical evaluation of re-coupling coefficients of increasing complexity has been developed over the last 20 years. The introduction to

the tables of RBMW59 includes a comprehensive bibliography of the literature dealing with the evaluation of coefficients involving the recoupling of not more than five angular momenta. Fano and Racah (FR59) have indicated the method of reduction of a recoupling coefficient of arbitrary complexity to sums of products of simpler coefficients. In particular, the diagrammatic methods of YLV62 have provided guidance for the classification and evaluation of coefficients which depend upon many j quantum numbers. A general computer program has recently been provided by Burke (B70) for the evaluation of any recoupling coefficient. At the end of Sec. 6 we shall show how the recoupling coefficient represented by the diagram in (3.7) may be obtained. The recoupling coefficient is exactly that given by the orbiton method of F65 and may be evaluated using Burke’s program. This procedure for the evaluation of the \mathcal{g} diagram may be used as an alternative to the graphical method which is given below.

In this section we describe the essential procedures that are utilized by computer programs. We do this by graphical methods derived from YLV62. The summation over M on the rhs of (4.2) is represented graphically by contracting the open lines on the rhs and lhs of the diagram in (3.7). The resulting form of \mathcal{g} has *no further open lines*. Moreover the contraction applies separately for the spin and orbital total angular momenta, i.e.,

$$\mathcal{g} = \delta(LL') \delta(SS') ([L][S])^{-1}$$



(4.3)

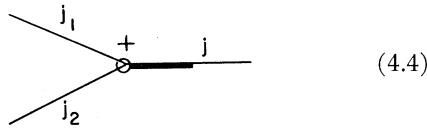
4.1 THE COUPLING SCHEMES

In an LS scheme of coupling, the spin and orbital momenta are coupled separately. This means that the diagram \mathcal{g} factors into a product of an orbital diagram and a spin diagram, i.e., $\mathcal{g} = \mathcal{L} \times \mathcal{S}$.

The orbital diagram \mathcal{L} is the \mathcal{g} diagram with all lines labeled with the corresponding orbital momenta. The spin diagram \mathcal{S} is the same diagram labeled with the corresponding spin momenta, except that, since the Coulomb interaction is *spin independent*, the k line together with the nodes at its ends is omitted. However, since most of the following procedure is applicable to both spin and orbital diagrams, for the moment we will continue to work with the composite diagram \mathcal{g} . For brevity, we will use the label j when we wish to refer to either spin or orbital momentum.

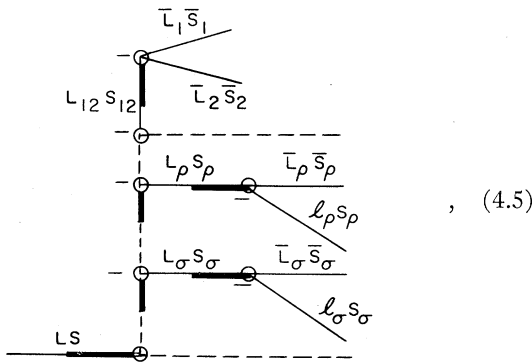
For the numerical evaluation of the recoupling coefficient, i.e., the closed diagram, it is necessary to specify explicitly the coupling schemes α, α' of the many-electron wave functions which have hitherto been denoted by blocks in the g diagram.

Algebraically, the coupling scheme is specified by a particular product of C-G coefficients summed over appropriate magnetic quantum numbers. Graphically, each C-G coefficient $(j_1 m_1 j_2 m_2 | j m)$ is represented by a graph with one node



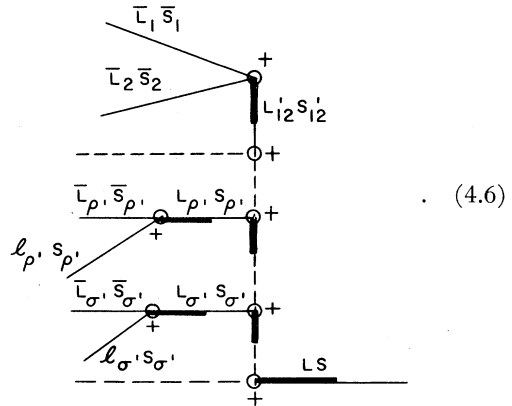
and the summation over magnetic quantum numbers is represented by joining appropriate free lines in the product of graphs like (4.4). This was the procedure used in Sec. 2.1 in representing the Coulomb interaction operator graphically.

In Sec. 2.2 we prescribed that the lines representing successive subshells of electrons be ordered vertically downwards in drawing the graphs. This convention means that, in the usual situation where subshell momenta are coupled sequentially, all nodes in the graph of the left-hand wave function have a $-$ sign (clockwise ordering of the first and second factor in a product) and all nodes in the graph of the right-hand wave function have a $+$ sign (anticlockwise ordering). For example, the scheme α which has the subshells coupled sequentially and the interacting electrons in subshells ρ and σ is drawn



where the dashed lines indicate intervening subshells of spectator electrons. Similarly, the scheme α' which has

the subshells coupled sequentially and interacting electrons in subshells ρ', σ' is drawn,

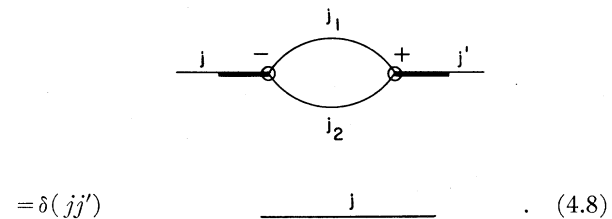


The "state graphs" (4.5) and (4.6) are contracted with the appropriate interaction graph to form the g diagram as was done in Sec. 3.1 to obtain the diagram in (3.7).

Simplifications can often be made in drawing the state graphs (4.5) and (4.6). Any closed subshells of spectator electrons may simply be ignored in the schemes α, α' because a closed subshell has total $L=0$, total $S=0$. Further, any groups of spectator subshells which precede *all* of the interacting subshells $\rho\rho'\sigma\sigma'$ may be replaced by their resultant momenta. This result follows from the orthonormality of C-G coefficients

$$\sum_{m_1 m_2} (j m | j_1 m_1 j_2 m_2) (j_1 m_1 j_2 m_2 | j' m') = \delta(j j') \delta(m m'), \tag{4.7}$$

which is represented graphically by



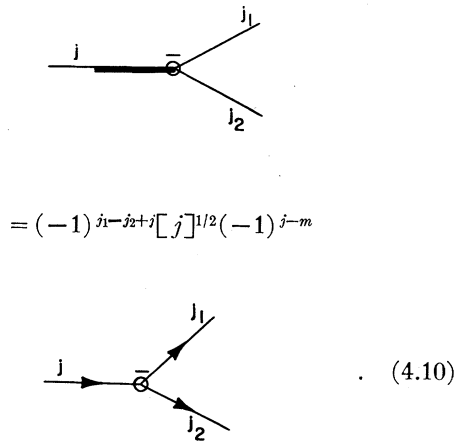
For example, in the contraction of (4.5) and (4.6), subshells 1 and 2 could be replaced by a single resultant line $L_{12} S_{12}$. This replacement does not affect the results of Sec. 3.2 since groups of spectator subshells which precede all interacting subshells do not contribute to the weight factor or Pauli phase factor.

4.2 The j -Coefficient Diagrams

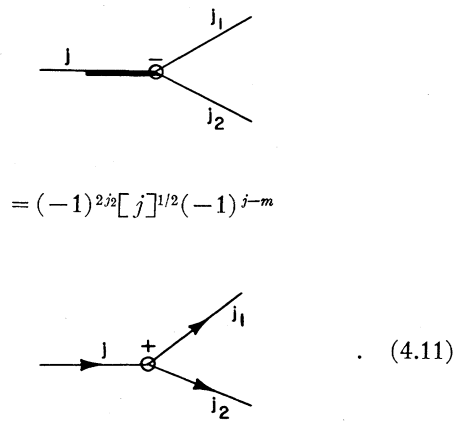
For graphical evaluation it is desirable to work with j coefficients, i.e., products of 3- j coefficients summed over all magnetic quantum numbers, rather than recoupling coefficients which are products of C-G coefficients summed over all magnetic quantum numbers. This is because the j coefficients are more symmetric under permutation of their arguments. The necessary transformation is achieved by replacing each C-G coefficient by the corresponding 3- j coefficient. For each node on the left-hand side we have

$$(jm | j_1 m_1 j_2 m_2) = (-1)^{j_1 - j_2 + j} [j]^{1/2} (-1)^{j-m} \begin{pmatrix} j_1 & j_2 & j \\ m_1 & m_2 & -m \end{pmatrix} \quad (4.9)$$

or graphically



We will also use the alternative form

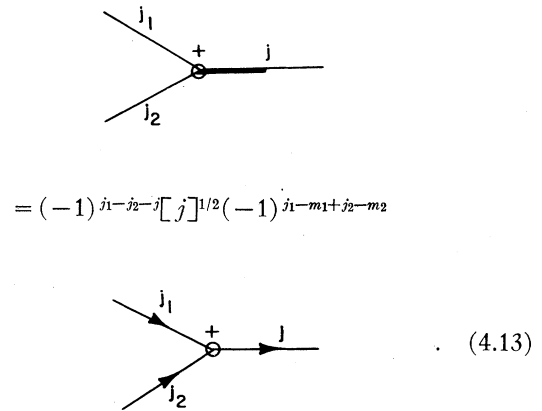


In drawing the right-hand side of (4.10) we have followed the convention of YLV62 that the sign of the magnetic quantum number in a 3- j coefficient is indicated by an arrow on the appropriate line. For a minus sign the arrow enters the node, and for a plus sign the arrow leaves the node. The 3- j coefficient is invariant under cyclic (even) permutation of its arguments and is multiplied by $(-1)^{j_1 + j_2 + j}$ under odd permutation of its arguments. Correspondingly, in the graphical representation of the 3- j coefficient, a change in the cyclic order of the momenta (i.e., a change in the sign on the node) is equivalent to multiplication by a factor $(-1)^{j_1 + j_2 + j}$. This property and the fact that $(j_1 + j_2 + j)$ is integral has been used in deriving (4.11).

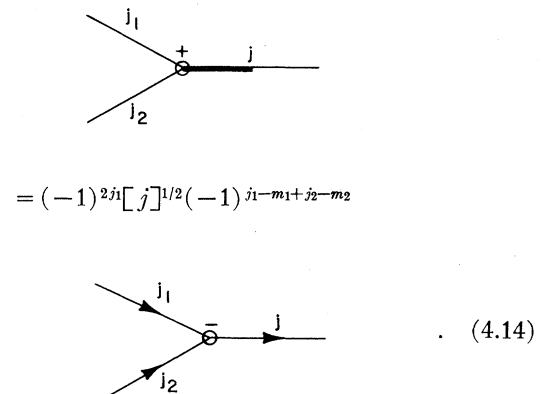
In a similar way, for each node on the right-hand side we make the substitution

$$(j_1 m_1 j_2 m_2 | jm) = (-1)^{j_1 - j_2 - j} \times [j]^{1/2} (-1)^{j_1 - m_1 + j_2 - m_2} \begin{pmatrix} j_1 & j_2 & j \\ -m_1 & -m_2 & m \end{pmatrix} \quad (4.12)$$

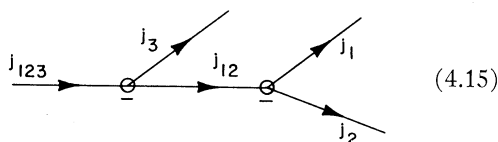
which is represented graphically as



Again we will use the alternative form



In the graphs of 3- j coefficients the joining of two free lines labeled with the same j and with similarly directed arrows corresponds to summing the product of the two 3- j coefficients with the factor $(-1)^{j-m}$. The magnetic quantum number m has opposite sign in the two coefficients. For example, the graph



corresponds to the summation

$$\sum_{m_{12}} (-1)^{j_{12}-m_{12}} \begin{pmatrix} j_1 & j_2 & j_{12} \\ m_1 & m_2 & -m_{12} \end{pmatrix} \begin{pmatrix} j_3 & j_{12} & j_{123} \\ m_3 & m_{12} & -m_{123} \end{pmatrix} \quad (4.16)$$

The right-hand side of (4.11) and (4.14) are designed so as to provide the $(-1)^{j-m}$ factors just where required to carry out the summations implied by joining the open lines. Since m is an index of summation, one can verify that changing the direction of an arrow on a closed line j is equivalent to changing m into $-m$ and hence to multiplication by a factor $(-1)^{2m} = (-1)^{2j}$.

The transformation of the diagrammatic representation of a recoupling coefficient, formed by contracting (4.5) and (4.6) with the interaction graph, to the diagram of a j coefficient is made by using the relations (4.11) and (4.14). The fact that all orbital momenta are integral means that the transformation of the orbital diagram becomes trivial. The first step in the transformation is

(i) separate the spin and orbital diagrams in the manner indicated at the beginning of Sec. 4.1.

For the spin diagram the transformation is completed by the following procedure:

(ii) introduce an arrow on each line of the state graphs (4.5) and (4.6). For the nodes of the left-hand state graph, each thick line has an arrow entering the node; each thin line has an arrow leaving the node. For the right-hand state graph, arrows on thick lines leave the nodes and arrows on thin lines enter the nodes. This means that, in the contracted graph, lines flow through the diagram all in the same direction.

The phase factors introduced by the transformations (4.11) and (4.14) are of the form $(-1)^{2j}$ and so may be canceled by reversal of the direction of appropriate arrows on the closed diagram. Hence we have the next

step³:

(iii) reverse the direction of the arrows on all lines in the spin diagram which appear as “2nd coupled” at each node of the diagram of the left-hand wave function and as “1st coupled” at each node of the diagram of the right-hand wave function. For some lines this may involve two such reversals, in which case they cancel.

The change of orientation of the nodes in the transformations (4.11) and (4.14) is achieved by the following step:

(iv) reverse the signs on all nodes in the spin diagram. Finally, the factors $[j]^{1/2}$ are included:

(v) multiply each diagram by a factor $[j]^{1/2}$ for each thick line j and then omit all “thick-line” labeling in accordance with (4.11) and (4.14).

For the orbital diagram, the transformation to a j coefficient diagram involves only step (v); steps (ii) and (iii) are unnecessary since all factors $(-1)^{2j}$ are positive for orbital momenta, i.e., arrows are not required on orbital diagrams. Further, for a closed orbital diagram, changing the signs of all nodes is equivalent to multiplication by the positive factor $(-1)^{2x}$, where x is the sum of all the momenta. Hence, step (iv) is also unnecessary.

The total L line and the total S line each have two thick portions so that step (v) gives a factor $[L][S]$ which cancels the factor $([L][S])^{-1}$ introduced in (4.3).

The spin and orbital diagrams now represent j coefficients.

Henceforth the diagrams may be deformed at will, subject only to the rule that if the deformation changes the cyclic ordering of momenta at a node, the sign on that node is reversed.

4.3 Reduction of Diagrams

The spin and orbital diagrams are now evaluated separately. The goal of diagrammatic evaluation is to reduce the diagram to a product (or sum of products) of

(a) standard irreducible diagrams of two kinds: (i) the “unit diagram” representing the triangular delta $\Delta(j_1 j_2 j_3)$,⁴ which is unity if $j_1 j_2 j_3$ form a triad (i.e., a node) and zero otherwise, and (ii) the diagram which represents the 6- j coefficient,

(b) weight factors of the type $[j]^{1/2}$,

(c) phase factors of the type $(-1)^\Phi$, where $\Phi = \sum_i j_i$.

The triangular delta $\Delta(j_1 j_2 j_3)$ is simply the orthogonality relation (4.7) averaged over all orientations,

³ This procedure is an alternative to that given in Sec. 22 of YLV62: it has the advantage that the correct phase to be associated with the diagrams is obtained by purely graphical operations.

⁴ Strictly speaking, the triangular delta is the “3- j coefficient” in the hierarchy of $3n$ - j coefficients. However we will adopt the common usage and reserve this name for the “Wigner” 3- j coefficient which appears, for example, on the right of (4.9).

i.e.,

$$\Delta(j_1 j_2 j_3) = \sum_{m_1 m_2 m_3} [j_3]^{-1} (j_3 m_3 | j_1 m_1 j_2 m_2) (j_1 m_1 j_2 m_2 | j_3 m_3). \quad (4.17)$$

Using the transformations (4.10) and (4.13) we have

$$\Delta(j_1 j_2 j_3) = (-1)^{2j_1+2j_2} \sum_{m_1 m_2 m_3} (-1)^{j_1-m_1+j_2-m_2+j_3-m_3}$$

The diagram shows two nodes. The left node is a circle with a minus sign, and three arrows labeled j_1 , j_2 , and j_3 meet at it. The right node is a circle with a plus sign, and three arrows labeled j_1 , j_2 , and j_3 meet at it. Below these is an equals sign followed by a loop diagram with three arrows labeled j_1 , j_2 , and j_3 forming a closed path. The loop starts with a minus sign and ends with a plus sign. Equation (4.18) is written to the right.

Since $j_1+j_2+j_3$ is an integer, this diagram is unchanged by reversing both signs or by reversing all three arrows.

The 6- j coefficient is a sum over a product of four 3- j coefficients, i.e.,

$$\begin{aligned} & \begin{Bmatrix} j_1 & j_2 & j_3 \\ l_1 & l_2 & l_3 \end{Bmatrix} \\ &= \sum_{m_i} (-1)^\Phi \begin{pmatrix} j_1 & j_2 & j_3 \\ m_1 & m_2 & m_3 \end{pmatrix} \begin{pmatrix} j_1 & l_2 & l_3 \\ -m_1 & -n_2 & n_3 \end{pmatrix} \\ & \times \begin{pmatrix} j_2 & l_3 & l_1 \\ -m_2 & -n_3 & n_1 \end{pmatrix} \begin{pmatrix} j_3 & l_1 & l_2 \\ -m_3 & -n_1 & n_2 \end{pmatrix}, \quad (4.19) \end{aligned}$$

where

$$\Phi = j_1 - m_1 + j_2 - m_2 + j_3 - m_3 + l_1 - n_1 + l_2 - n_2 + l_3 - n_3.$$

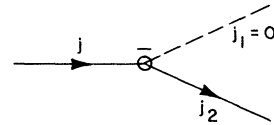
Diagrammatically, the 6- j coefficient is represented by

The diagram shows a triangle with three vertices, each marked with a plus sign. The edges are labeled with l_1 , l_2 , and l_3 . At each vertex, two edges meet, and the third edge is labeled with j_1 , j_2 , and j_3 respectively. Equation (4.20) is written to the right.

The full symmetry of (4.19) and (4.20) under per-

mutation of triads can be verified. Any diagram or subdiagram which is obtained with the same structure as (4.20) but with alternative nodal signs and arrow orientation may be put in the standard form. A factor $(-1)^{j_1+j_2+j_3}$ must be included for each reversal of a nodal sign and a factor $(-1)^{2j}$ for each arrow reversal. The phase factor introduced in this way will be called the *geometric* phase factor.

The techniques for reducing closed diagrams to sums of products of diagrams like (4.18) and (4.20) mirror the algebraic expansion of the j coefficients into sums of products of 6- j coefficients. A preliminary simplification is to erase any line corresponding to $j=0$. This erasure leaves two nodes at which only two lines meet. These nodes may be removed by the transformation

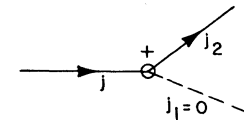


$$= [j]^{-1/2} \delta(j_2 j) \quad \longrightarrow \quad j \quad (4.21)$$

which derives from the relation

$$(jm | 00j_2 m_2) = \delta(j_2 j) \delta(m_2 m). \quad (4.22)$$

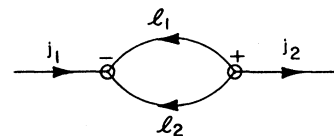
By changing the orientation of the node in (4.21), we have the alternative form,



$$= [j]^{-1/2} \delta(j_2 j) \quad \longrightarrow \quad j \quad (4.23)$$

Any node involving a zero line in a closed diagram may be brought to the form of the left-hand side of (4.21) or (4.23) by reversing arrows and including the appropriate phase factors.

Any closed loops can also be removed at the outset by use of the orthonormality relation (4.8), which in terms of j -coefficient graphs is



$$= \delta(j_1 j_2) [j_1]^{-1} \quad \longrightarrow \quad j_1 \quad (4.24)$$

The basic idea of the diagrammatic reduction is that if two parts of a closed graph, each containing more than one node, are connected by a single line, that line must have $j=0$ owing to the invariance under rotations. The diagram then splits into two parts by erasure of the connecting line and removal of the two nodes involved according to (4.21) or (4.23), i.e.,

The diagram shows two rectangular blocks, α and α' , connected by a single line. On the left, two lines with arrows labeled j_1 and j_2 enter a node with a plus sign. A line with an arrow labeled $j=0$ connects this node to another node with a minus sign on the right. From this second node, two lines with arrows labeled j'_1 and j'_2 exit to block α' . Below this is the equation:

$$= [j_1]^{-1/2} [j'_1]^{-1/2} \delta(j_1 j_2) \delta(j'_1 j'_2)$$

Below the equation is a diagram showing two separate blocks, α and α' , each with a curved arrow on its side. The arrow on α is labeled j_1 and the arrow on α' is labeled j'_1 . The two diagrams are separated by a multiplication sign \times . To the right of this diagram is the label (4.25).

Again, a diagram with the same topology can always be made identical to the left-hand side of (4.25) by suitable reversal of arrows and signs.

The first step is to determine the minimum number of lines which must be cut to separate the diagram into two parts, each containing more than one node. If only one line need be cut, then (4.25) is applied. If two or more lines connect two parts of the same diagram, we can always reduce to the form of the left-hand side of (4.25) by successive application of the expansion

The diagram shows two rectangular blocks, α and α' , connected by two parallel lines with arrows labeled j_1 and j_2 . Below this is the equation:

$$= \sum_j [j]$$

Below the equation is a diagram showing two separate blocks, α and α' , each with a node. A line with an arrow labeled j connects the node in α to the node in α' . The node in α has a plus sign and the node in α' has a minus sign. A dashed line connects the two nodes. To the right of this diagram is the label (4.26).

where the dashed line indicates any number of other connecting lines. This expansion derives from the second

orthonormality property of the C-G coefficients, i.e.,

$$\delta(m_1 m'_1) \delta(m_2 m'_2) = \sum_{jm} (j_1 m_1 j_2 m_2 | jm) (jm | j'_1 m'_1 j'_2 m'_2). \quad (4.27)$$

The expansion (4.26) may be verified by the substitution of the transformations (4.10) and (4.13) in (4.27). Note that the signs on the nodes in (4.26) are only required to be different since reversal of both introduces a factor $(-1)^{2j_1+2j_2+2j}$ which is positive.

The first corollary of (4.26) is that if a diagram is separable on two lines, then, from (4.25), only the $j=0$ term is allowed. The result is

The diagram shows two rectangular blocks, α and α' , connected by two parallel lines with arrows labeled j_1 and j_2 . Below this is the equation:

$$= [j_1]^{-1} \delta(j_1 j_2)$$

Below the equation is a diagram showing two separate blocks, α and α' , each with a curved arrow on its side. The arrow on α is labeled j_1 and the arrow on α' is labeled j'_1 . The two diagrams are separated by a multiplication sign \times . To the right of this diagram is the label (4.28).

Note that the arrows in the diagram on the left-hand side of (4.28) are in directions such that, after cutting the lines j_1 and j_2 , the arrows on lines connected to the same block have the relative direction necessary for their joining to form the product of diagrams on the right-hand side.

The second corollary of (4.26) is the application to a diagram separable on three lines. Here two summations are introduced:

The diagram shows two rectangular blocks, α and α' , connected by three parallel lines with arrows labeled j_1 , j_2 , and j_3 . Below this is the equation:

$$= \sum_j \sum_{j'} (-1)^{2j} [j] [j'] \times$$

Below the equation is a diagram showing two separate blocks, α and α' , each with a node. A line with an arrow labeled j connects the node in α to the node in α' . The node in α has a plus sign and the node in α' has a minus sign. A dashed line connects the two nodes. To the right of this diagram is the label (4.29).

Owing to (4.25), j' must vanish. Moreover, (4.23) then requires that $j=j_3$ so that the summation over j and j' in (4.29) disappears. The final result is that a diagram separable on three lines is expressible as a simple product, i.e.,

(4.30)

Since no more than three lines meet at one node, clearly three is the maximum number of lines on which a diagram may be separable in order to be expressible as a simple product of two diagrams.

In the general case of a diagram separable on no less than n lines, $(n-3)$ intermediate summations (4.26) are necessary for reduction to a diagram separable on three lines, to which (4.30) may then be applied. Again, any diagram separable on three lines may be brought to the form of the left-hand side of (4.30) by the reversal of arrows. Also, the requirement is only that the signs on the nodes on the right-hand side of (4.30) be different since reversing both signs involves the positive phase factor $(-1)^{2j_1+2j_2+2j_3}$.

Once a graphical representation of a j coefficient has been obtained in accordance with steps (i)–(v) of Sec. 4.1, its numerical evaluation is carried out by devising a sequence of operations which breaks it up into components no larger than the $6-j$ coefficient (4.20). Each operation will be one of those represented by the sequence (4.21), (4.24), (4.25), (4.28), and (4.30) or the introduction of an intermediate summation by use of (4.26). The result will be a product, or sum of products of diagrams representing the $6-j$ coefficient (4.20) or the triangular delta (4.19). For very large diagrams, where there may be alternative sequences of

reduction, a method of choosing the most efficient sequence, i.e., the one involving the minimum number of intermediate summations has been derived (RBY65). This method is described in detail by Bordarier (Bo70). The final step is the numerical evaluation of the diagrams representing $6-j$ coefficients. The numerical values of the $6-j$ coefficients have been tabulated extensively by Rotenberg *et al.* (RBMW59). Computer subroutines for their evaluation are widely available.

4.4 Examples

As specific examples of the application of the procedure of Secs. 4.1–4.3, we will consider the evaluation of the recoupling coefficients of quintuple products of angular momenta of resultant zero. The graphical representation of the recoupling coefficients involves the contraction of diagrams like (4.5) and (4.6). Of course, the interaction graphs do not appear, but these do not figure in the procedure of Sec. 4.2.

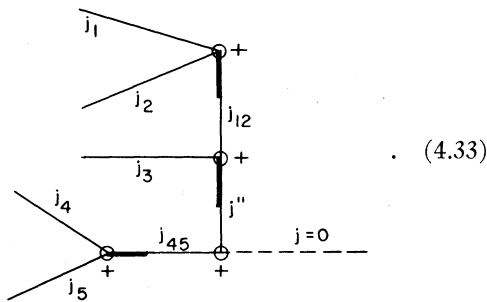
According to Chapter XII of Fano and Racah (FR59), the transformations of quintuple products of degree zero fall into three groups characterized by the recoupling coefficients

$$\begin{aligned}
 R_1 &\equiv ((j_1 j_2)j_{12}, (j_3 j_4)j_{34}, j_5 \mid (j_1 j_2)j_{12}, j_3, (j_4 j_5)j_{45})^{(0)}, \\
 R_2 &\equiv ((j_1 j_2)j_{12}, (j_3 j_4)j_{34}, j_5 \mid j_1, (j_2 j_3)j_{23}, (j_4 j_5)j_{45})^{(0)}, \\
 R_3 &\equiv ((j_1 j_2)j_{12}, (j_3 j_4)j_{34}, j_5 \mid (j_1 j_3)j_{13}, (j_2 j_4)j_{24}, j_5)^{(0)}.
 \end{aligned}
 \tag{4.31}$$

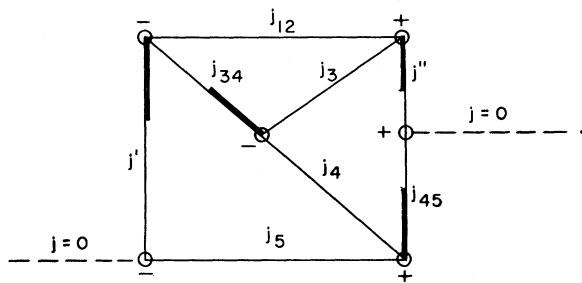
In terms of C–G coefficient diagrams, the left-hand side of the recoupling coefficient R_1 is represented by the diagram

(4.32)

and the right-hand side by

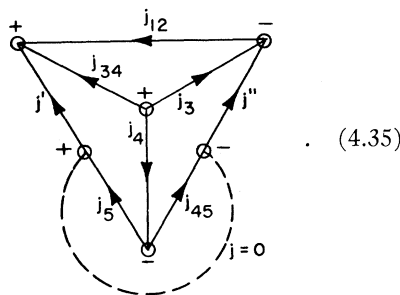


Upon contraction of (4.32) and (4.33), the lines j_1 and j_2 form a closed loop which is removed by the use of (4.8) to leave the diagram



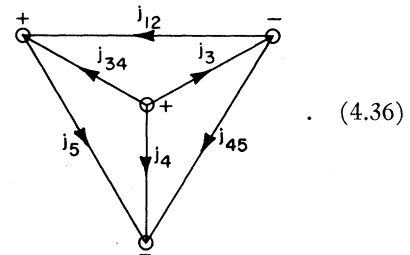
The angular momenta involved in (4.31) may be half-integral so that in transforming (4.34) to a j -coefficient diagram we must follow the procedure given in Sec. 4.2 for the spin diagram. Application of the procedures of steps (ii), (iii), (iv), and (v) of Sec. 4.2 converts diagram (4.34) to the diagram of a j coefficient. The result is

$$R_1 = ([j'] [j_{34}] [j''] [j_{45}])^{1/2} \times$$



The two nodes involving the $j=0$ line can be removed by application of (4.23) to give

$$R_1 = ([j_{34}] [j_{45}])^{1/2} \times$$



Reversal of the signs of the two minus nodes in this diagram and reversal of the arrow on the j_{45} line give the diagram of the 6- j coefficient

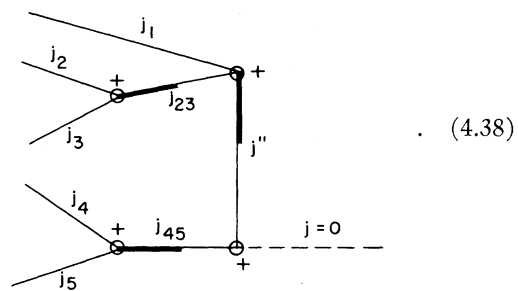
$$\begin{Bmatrix} j_3 & j_4 & j_{34} \\ j_5 & j_{12} & j_{45} \end{Bmatrix}$$

multiplied by the phase factor $(-1)^{j_3+j_4+j_5+j_{12}}$.

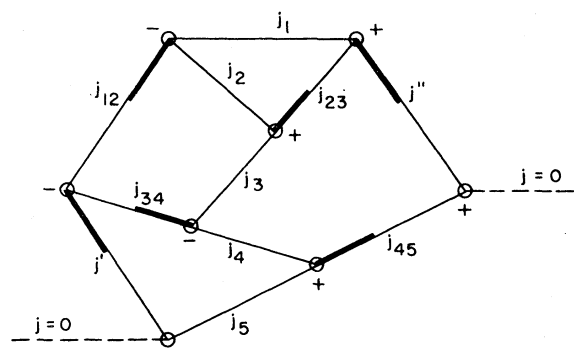
Finally, we have the result

$$\begin{aligned} R_1 &\equiv (j_{12} j_{34} j_5 | j_{12} j_3 j_{45})^{(0)} \\ &= (j_{34} j_5 | j_3 j_{45})^{(j_{12})} \\ &= (-1)^{j_3+j_4+j_5+j_{12}} [j_{34}]^{1/2} [j_{45}]^{1/2} \begin{Bmatrix} j_3 & j_4 & j_{34} \\ j_5 & j_{12} & j_{45} \end{Bmatrix}. \end{aligned} \quad (4.37)$$

The right-hand side of R_2 is represented by



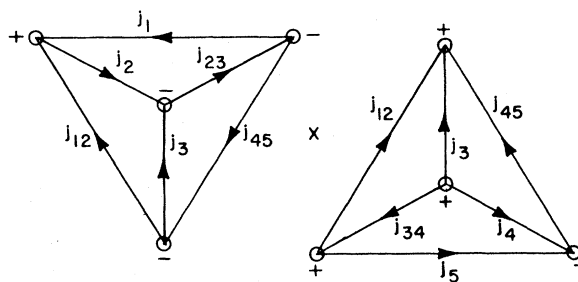
Contraction of this diagram with the diagram (4.32) shown to be equal to the product of the left-hand side gives the diagram



(4.39)

Application of steps (ii), (iii), (iv), and (v) of Sec. (4.2) and subsequent removal of the nodes involving the \$j=0\$ lines converts (4.39) to a \$j\$-coefficient diagram. The result is

$$R_2 = ([j_{12}][j_{34}][j_{23}][j_{45}])^{1/2}$$

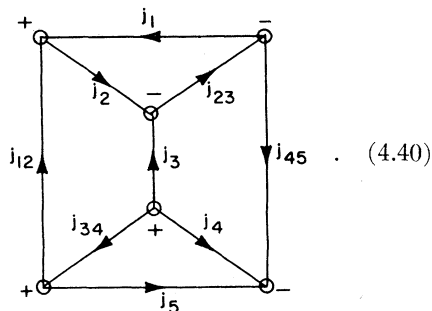


(4.41)

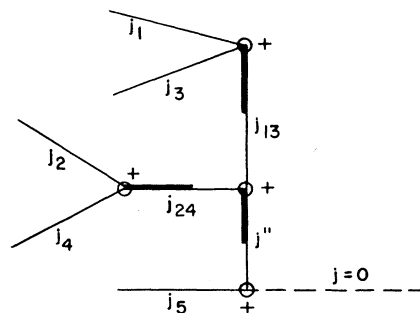
Each of the diagrams in (4.41) can be brought to the standard form (4.20) of the 6-\$j\$ coefficient by reversal of appropriate nodes and arrows. Finally, we obtain the result

$$R_2 \equiv (j_{12} j_{34} j_5 | j_1 j_{23} j_{45})^{(0)} = (-1)^{j_1+j_2+j_3+j_4+j_5+j_{12}} ([j_{12}][j_{23}][j_{45}][j_{34}])^{1/2} \times \begin{Bmatrix} j_3 & j_2 & j_{23} \\ j_1 & j_{45} & j_{12} \end{Bmatrix} \begin{Bmatrix} j_3 & j_4 & j_{34} \\ j_5 & j_{12} & j_{45} \end{Bmatrix}. \quad (4.42)$$

For the third type of recoupling coefficient \$R_3\$, the left-hand side is given by (4.32) and the right-hand side by



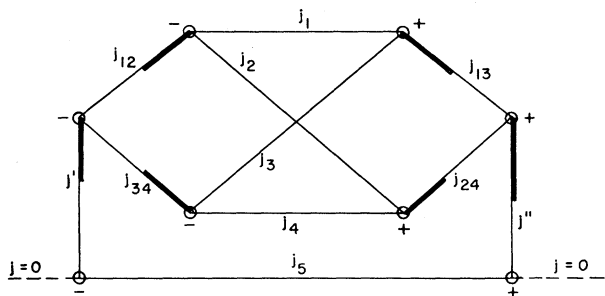
(4.40)



(4.43)

The diagram in (4.40) separates on the three lines \$j_{12}\$, \$j_3\$, and \$j_{45}\$. Using the result (4.30), the diagram is

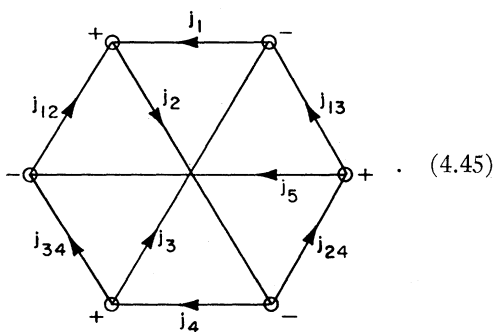
Contraction of (4.43) with (4.32) gives the diagram



(4.44)

Application of steps (ii), (iii), (iv), and (v) of Sec. 4.2 and removal of the nodes involving the $j=0$ lines converts (4.44) to a j -coefficient diagram. The result is

$$R_3 = ([j_{12}][j_{34}][j_{13}][j_{24}])^{1/2}$$

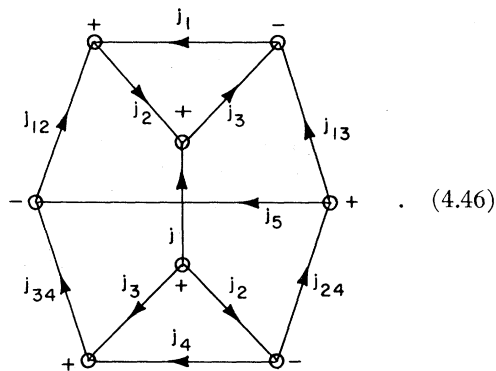


(4.45)

The diagram in (4.45) is separable on a minimum of four lines. Therefore we apply (4.26) to two lines of

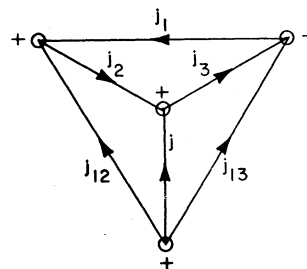
the four, for example, j_2 and j_3 . This gives

$$R_3 = ([j_{12}][j_{34}][j_{13}][j_{24}])^{1/2} \sum_j [j]$$

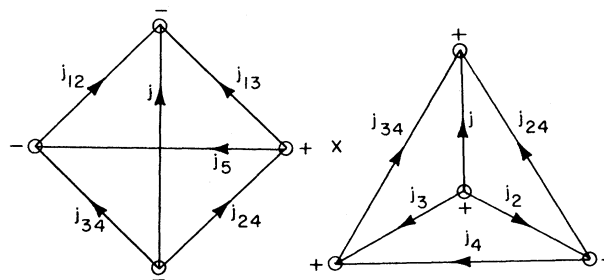


The diagram in (4.46) is separable on the three lines j_2, j_3, j_4 and again on the three lines j_{34}, j, j_{24} . Application of (4.30) to each set of three lines gives a product of three diagrams, i.e.,

$$R_3 = ([j_{12}][j_{34}][j_{13}][j_{24}])^{1/2} \sum_j [j]$$



×



(4.47)

The second diagram is redrawn in “tetrahedral” form and each diagram brought to the form (4.30) by suitable change of nodal signs and reversal of arrows. This procedure leads to the final result

$$R_3 = (j_{12} j_{34} | j_{13} j_{24})^{(j_5)} = ([j_{12}][j_{34}][j_{13}][j_{24}])^{1/2} (-1)^S \sum_j [j] (-1)^{2j} \times \left\{ \begin{matrix} j & j_3 & j_2 \\ j_1 & j_{12} & j_{13} \end{matrix} \right\} \left\{ \begin{matrix} j & j_{34} & j_{24} \\ j_5 & j_{13} & j_{12} \end{matrix} \right\} \left\{ \begin{matrix} j & j_3 & j_2 \\ j_4 & j_{24} & j_{34} \end{matrix} \right\} \quad (4.48)$$

where $S = (j_1 + j_2 + j_3 + j_4 + j_5 + j_{12} + j_{34} + j_{13} + j_{24})$, i.e., is equal to the sum of the 9 momenta in diagram (4.45).

The recoupling coefficient R_3 is used to define the 9- j coefficient (FR59), i.e.,

$$(j_{12} j_{34} | j_{13} j_{24})^{(j_5)} = ([j_{12}][j_{34}][j_{13}][j_{24}])^{1/2} \times \left\{ \begin{matrix} j_1 & j_2 & j_{12} \\ j_3 & j_4 & j_{34} \\ j_{13} & j_{24} & j_5 \end{matrix} \right\}. \quad (4.49)$$

By comparison of (4.49) and (4.48) we obtain an expansion of the 9- j coefficient in terms of 6- j coefficients.

From the right-hand sides of (4.49) and (4.45) we can see that the diagram in (4.45) is a representation of the 9- j coefficient. Where appropriate computer routines or tables of 9- j coefficients are available, it may be convenient to use this diagram as a “standard” diagram.

5. MULTIPOLE OPERATORS

In this section we will evaluate the matrix element of the multipole transition operator (2.12). This matrix element is not diagonal in the total angular and magnetic quantum numbers of the states, i.e., is of the form

$$T = (A, \alpha L S J M | \sum_i r_i^k C_q^{[k]}(\Omega_i) | B, \alpha' L' S' J' M'). \quad (5.1)$$

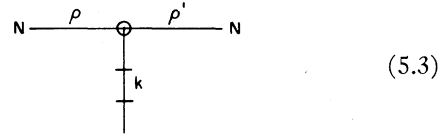
The matrix element of a one-electron operator vanishes unless the configurations A and B differ at most by the nl quantum numbers of a single electron. When the configurations differ in the quantum numbers of a single electron, the sum over λ, λ' in (2.12) is restricted to the pair of subshells which differ in their occupation number $N_\lambda, N_{\lambda'}$ in A and B . When the configurations are the same, there are alternative choices $\lambda = \lambda'$ of the interacting subshells. However, as for the Coulomb operator, the contribution $T(\lambda\lambda')$ of the matrix element of each nonzero term in (2.12) may be calculated separately, i.e., $T = \sum_{\lambda\lambda'} T(\lambda\lambda')$. We will consider the contribution of one term $T(\rho\rho')$.

5.1 Integration over Electron Variables

Each term in the sum over i in (5.1) contributes equally to the matrix element. Designating the N th electron as the interacting electron we have

$$T = N (A, \alpha L S J M | r_N^k C_q^{[k]}(\Omega_N) | B, \alpha' L' S' J' M'). \quad (5.2)$$

The matrix element $T(\rho\rho')$ is obtained by bracketing the operator



with the many-electron wave functions

$$\mathfrak{Y}^{-1/2} \sum_a (-1)^{P_a} \quad (5.4)$$

and

$$\mathfrak{Y}'^{-1/2} \sum_{q'} (-1)^{P_{q'}} \quad (5.5)$$

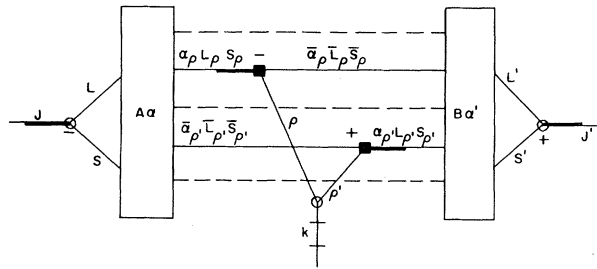
The orthogonality of one-electron wave functions requires each spectator electron to remain in the same subshell. Therefore, only those distributions q, q' having electron N in the ρ subshell on the left and in the ρ' subshell on the right and with the same distribution \bar{q} of spectator electrons give a nonzero result upon con-

traction of the state graphs (5.4) and (5.5) with the interaction graph (5.3). Each term in the sum over q, q' which is diagonal in the distribution of spectator electrons contributes equally. We will consider one such distribution and multiply by the number \mathfrak{N} of different distributions, where

$$\mathfrak{N} = (N-1)! / (\Pi \bar{N}_\lambda!) \quad (5.6)$$

The interacting electron N is separated from other electrons in the same subshell (ρ on the left and ρ' on the right) by the f.p. expansion (2.18). Contraction of the state graphs with the interaction graph (5.3) gives the result

$$T(\rho\rho') = N(\mathfrak{N}\mathfrak{N}')^{-1/2} \bar{\mathfrak{N}} (-1)^{P_A+P_B} \times \sum_{\text{f.p.}}$$



(5.7)

The weight factor for the term $T(\rho\rho')$ is

$$N(\mathfrak{N}\mathfrak{N}')^{-1/2} \bar{\mathfrak{N}} = (N_\rho N_{\rho'})^{1/2} \quad (5.8)$$

which again is just the square root of the number of electrons available for transfer out of each interacting subshell. The Pauli phase factor is simply the parity of the permutation necessary to transfer the N th electron into the subshell ρ in the left-hand state and ρ' in the right-hand state. As in (3.9) or (3.10) for the pair of interacting electrons, we have

$$P_A = \sum_{\lambda=\rho+1}^{\infty} \bar{N}_\lambda, \quad P_B = \sum_{\lambda=\rho'+1}^{\infty} \bar{N}_\lambda. \quad (5.9)$$

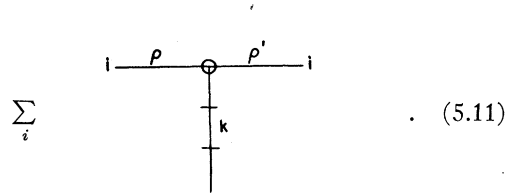
The right-hand side of (5.7) is multiplied by the relevant c.f.p. and the factor $I(k; \rho\rho')$ with simultaneous removal of the full squares and the double bar

from the k line, to give

$$T(\rho\rho') = (-1)^{P_A+P_B} (N_\rho N_{\rho'})^{1/2} I(k; \rho\rho') \times \sum_{\text{f.p.}} (l_\rho^N \alpha_\rho L_\rho S_\rho \{ | l_\rho^N \alpha_\rho^{-1} \bar{\alpha}_\rho \bar{L}_\rho \bar{S}_\rho, l_\rho \} \times (l_{\rho'}^{N'} \alpha_{\rho'}^{-1} \bar{\alpha}_{\rho'} \bar{L}_{\rho'} \bar{S}_{\rho'}, l_{\rho'} \} | l_{\rho'}^{N'} \alpha_{\rho'} L_{\rho'} S_{\rho'} \} \times \mathcal{G}. \quad (5.10)$$

Here, \mathcal{G} is the diagram in (5.7) with the full squares removed from the nodes and the double bar removed from the k line. The diagram \mathcal{G} is a function of angular momentum and magnetic quantum numbers only and is evaluated by the techniques of Sec. 4.

Where there are alternative choices of the interacting subshells, each term $T(\lambda\lambda')$ is evaluated in the form (5.10) and the partial results added. In the case of a one-electron operator there is only one term in the sum (2.12) for each set $\{\lambda\lambda'\}$ of interacting subshells. The curtailed operator is then just the appropriate term in the sum (2.12), e.g., the contribution $T(\rho\rho')$ given by (5.10) is the matrix element of the curtailed operator

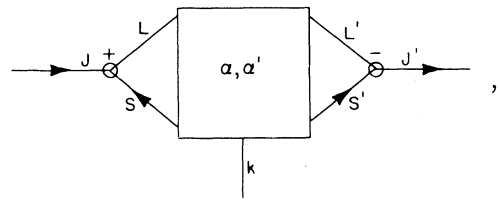


(5.11)

5.2 The Angular Factor

The evaluation of the diagram \mathcal{G} is complicated by the presence of the open line k which reflects the tensor nature of the operator. Application of the transformations (4.11) and (4.14) to the $(LS)J$ and $(L'S')J'$ nodes in the diagram \mathcal{G} gives

$$\mathcal{G} = (-1)^{J-M} [J]^{1/2} [J']^{1/2}$$



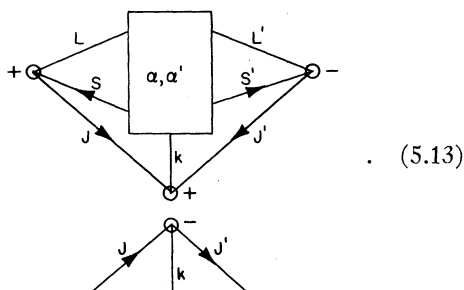
(5.12)

where the block α, α' denotes the rest of the diagram in (5.7) and does not concern us at this point.

The diagram in (5.12) has three open lines. By the same reasoning as led to (4.30), any such diagram can be expressed as a closed diagram (a j coefficient) and

the diagram of a 3- j coefficient, e.g.,

$$g = (-1)^{J-M} [J]^{1/2} [J']^{1/2}$$



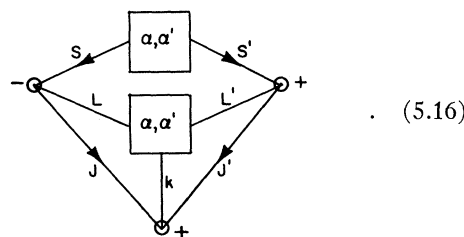
The open graph in (5.13) represents the 3- j coefficient

$$\begin{pmatrix} J' & k & J \\ M' & q & -M \end{pmatrix}. \quad (5.14)$$

The graphical procedure used to obtain (5.13) from (5.12) has been given by MEL67 and is a particular case of a general procedure for handling diagrams with open lines given in Sec. 14 of YLV62. In the case where there are three open lines, two labeled with the total momenta of angular wave functions and one with the rank of a tensor operator, the procedure is called the Wigner-Eckart theorem. Algebraically the Wigner-Eckart theorem is represented by the equation

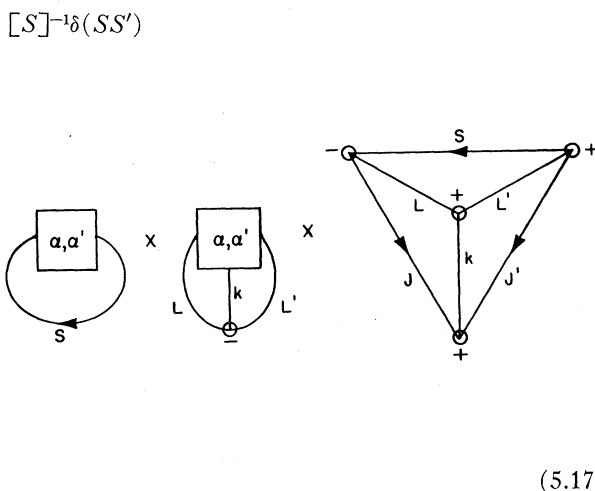
$$\begin{aligned} & (\alpha JM | T_q^{[k]} | \alpha' J' M') \\ &= (-1)^{J-M} \begin{pmatrix} J' & k & J \\ M' & q & -M \end{pmatrix} (-1)^{J'+k+J} \\ & \quad \times (\alpha J || T^{[k]} || \alpha' J'). \end{aligned} \quad (5.15)$$

Since spin and orbital momenta are coupled separately, the block (α, α') in the closed diagram on the right-hand side of (5.13) may be separated into two blocks, one representing the coupling of orbital momenta and the other representing the coupling of spin momenta. Since the interaction is spin independent, the k line is attached to the orbital block, i.e., the closed diagram becomes the diagram



Note that the signs on the LSJ and $L'S'J'$ nodes have been changed to compensate for the change in the orientation of these nodes between (5.13) and (5.16).

The diagram (5.16) can be separated firstly on the two lines S and S' and secondly on the three lines L, L', k . Application of (4.28) and (4.30) gives a product of three diagrams, i.e., the diagram (5.16) becomes



By reversing the sign of the LSJ node and the direction of the arrow on the J' line, the third diagram is brought to the form (4.20) of a 6- j coefficient. We will call the second diagram in (5.17) the orbital diagram \mathcal{E} and the first diagram the spin diagram \mathcal{S} . Note that the graphical procedure leading from (5.16) to (5.17) is equivalent to application of the standard formula (FR59)

$$\begin{aligned} (LSJ || T^{[k]} || L'S'J') &= [J]^{1/2} [J']^{1/2} (-1)^{L+S+k+J'} \delta(SS') \\ & \times \begin{Bmatrix} J & J' & k \\ L' & L & S \end{Bmatrix} (L || T^{[k]} || L'), \end{aligned} \quad (5.18)$$

where the operator $T^{[k]}$ operates in the orbital space only.

Finally upon substitution of (5.17) for the closed diagram in (5.13), we obtain the result

$$\begin{aligned} g &= [J]^{1/2} [J']^{1/2} (-1)^{J-M} \begin{pmatrix} J' & k & J \\ M' & q & -M \end{pmatrix} \\ & \times (-1)^{L-S+J} \begin{Bmatrix} L & L' & k \\ J' & J & S \end{Bmatrix} \delta(SS') [S]^{-1} \mathcal{E} \times \mathcal{S}. \end{aligned} \quad (5.19)$$

This result is then used to calculate g in Eq. (5.10) for the matrix element $T(\rho\rho')$. The diagrams \mathcal{E} and \mathcal{S} are then evaluated by the steps (i)-(v) of Sec. 4.2.

All factors in (5.19) other than the diagrams \mathcal{E} and \mathcal{S} are functions of total quantum numbers only and so are the same for all terms which contribute to the

matrix element T . This suggests that each term $T(\lambda\lambda')$ can be evaluated by initially ignoring the coupling of total L and S . The sum of all terms is then multiplied by the factors in (5.19) which involve J or J' . In this way, the state graphs (5.4) and (5.5) can be drawn with L and S uncoupled as in (2.15) and (2.16). After contraction with the interaction graph, the following diagram replaces g in (5.10) and (5.12),

$$g' \equiv \begin{array}{c} \text{---} LS \text{---} \boxed{\alpha, \alpha'} \text{---} L'S' \text{---} \\ | \\ k \end{array} \quad (5.20)$$

Joining the three lines in a node whose orientation represents the order LkL' and separation of spin and orbital diagrams give

$$g' = \delta(SS')[S]^{-1}$$

$$\begin{array}{c} \boxed{\alpha, \alpha'} \\ \circlearrowleft \\ S \end{array} \times \begin{array}{c} \boxed{\alpha, \alpha'} \\ | \\ k \\ \circlearrowright \\ L' \\ \ominus \\ L \end{array} \quad (5.21)$$

The factors $\delta(SS')[S]^{-1}$ arise because closure of the S, S' lines implies the application of (4.2). The diagrams in (5.21) are the \mathcal{L} and \mathcal{S} diagrams of (5.17). By comparison of (5.21) and (5.19) we see that g' includes all factors in g which do not depend upon the total angular momenta J and J' . This means that the results of the graphical procedure leading to (5.19) may be obtained by drawing the state graphs with L and S uncoupled as in (5.20), applying Eq. (5.21), and finally multiplying by the factors

$$(-1)^{J-M} \begin{pmatrix} J' & k & J \\ M' & q & -M \end{pmatrix} \times (-1)^{L-S+J} [J]^{1/2} [J']^{1/2} \begin{Bmatrix} L & L' & k \\ J' & J & S \end{Bmatrix}, \quad (5.22)$$

which involve the total J and J' quantum numbers. The factor

$$[J]^{1/2} [J']^{1/2} \begin{Bmatrix} L & L' & k \\ J' & J & S \end{Bmatrix}$$

is, to within a phase factor, the *line factor* of atomic spectroscopy, which has been tabulated by Menzel and Shore (MS68) for dipole transitions.

6. SUMMARIZED PRESCRIPTION

In this section the results of Secs. 2, 3, and 5 will be summarized in the form of a step-by-step procedure by which matrix elements of Coulomb or transition multipole operators may be evaluated. In this way the method of the previous sections may be considerably simplified. For example, in the graphs of Sec. 3, the open lines are labeled i, j, q_λ , etc., according to the electron or group of electrons whose wave function they represent. The purpose of this labeling is to enable the Pauli phase factor and the weight factor to be calculated, as is done in Sec. 3.2. After integration over all coordinates (i.e., contraction of the graphs) the labels no longer appear, of course. By giving a *prescription* for the calculation of the weight factor and Pauli phase factor, the electron labels need never be specified on the diagrams. Also, from the development which led to the curtailed form of the operators, we need consider only those graphs which are distinct in the pairs of subshells which are coupled by an interaction line.

6.1 Step-by-Step Procedure

The matrix element M [Eq. (3.2)] of the Coulomb operator or the matrix element T [Eq. (5.1)] of the transition multipole operator is evaluated by the procedure described in the following paragraphs.

(i) Identify the possible choices of subshells which contain interacting electrons as distinct from those which contain only spectator electrons. This is equivalent to enumerating the sets of subshells which give nonzero contributions $M(\lambda\mu\lambda'\mu')$ to M as described in Sec. 3.1, or nonzero contributions $T(\lambda\lambda')$ to T as described in Sec. 5.1. Each set of interacting subshells is characterized by a particular configuration of the spectator electrons. The configurations of spectator electrons are determined by the requirements (F65)

$$\bar{N}_\lambda \leq \min(N_\lambda, N_{\lambda'}) \quad (6.1)$$

and

$$\sum_\lambda \bar{N}_\lambda = N - n \quad (6.2)$$

for an n -electron operator. For a Coulomb operator, we have $n=2$; for a multipole operator, we have $n=1$. The possible choices of interacting subshells are listed, their contributions calculated separately and added at the end. We shall consider the contribution of the interaction between subshells ρ, σ on the left and ρ', σ' on the right for a Coulomb operator, or ρ on the left and ρ' on the right for a multipole operator.

(ii) Draw all distinct interaction graphs. This means all interaction graphs which are distinct in the pairs of subshells which are coupled by the interaction. In the case $\rho \neq \sigma, \rho' \neq \sigma'$ there are two such graphs; in all other cases there is only one interaction graph. This expresses the results of Sec. 3.2, where it was shown that the interaction between each set of subshells may be cal-

culated by using the curtailed form (3.12), (3.16), or (3.19) of the Coulomb operator. For a multipole operator each "set" of subshells is a single pair, so that clearly there is only one interaction graph, which is given in (5.11).

The Coulomb interaction graphs are drawn, as in (3.11a) and (3.11b), for example, with the open ends of the one-electron lines ordered vertically downwards. However, the electron labels $N-1$, N are omitted for the reasons discussed above. A cross is placed on the k lines in the Coulomb operator graphs and a double bar on the k line of the transition operator graph.

Each graph represents an operator whose matrix element is calculated by the procedure given below. In the case $\rho \neq \sigma$, $\rho' \neq \sigma'$ the contributions of the two graphs are calculated separately and the results added. We will consider the calculation of the matrix element of a single interaction operator graph.

In Sec. 7 we will consider sums of products of Coulomb and multipole operators which give rise to n -electron interaction operator graphs which may contain more than one interaction line. The interaction graphs representing a single Coulomb (two-electron) operator or a single multipole (one-electron) operator are particular cases of these n -electron graphs. Therefore, the procedure given below will refer to the evaluation of the matrix element of an n -electron interaction graph so as to be applicable also to the results of Sec. 7.

(iii) Multiply the interaction graph by a factor (-1) for each time that one-electron lines cross. This is in accordance with the phase rule established in Section (3.2).

(iv) Draw the state graphs representing the wave functions of the left-hand and right-hand states. These graphs are drawn as on the right-hand side of (2.15), with the interacting electrons separated from the spectator electrons in the same subshell as in the graphs on the right-hand side of (2.18) or (2.19). The coupling schemes α , α' need not be specified at this point and the electron labels i , j , q_λ , etc., can be omitted from these graphs. Closed shells of spectator electrons may be ignored. Lines representing groups of spectator electrons must be labeled with the same momenta $\bar{L}_\lambda \bar{S}_\lambda$ in the left-hand and right-hand state diagrams. Also, from the results of Sec. 4.1, the spectator subshells which precede in order *all* the interacting subshells $\rho \sigma \rho' \sigma'$ may be represented by a single line labeled with the same resultant momenta in both graphs.

The state graphs should be drawn with the resultant lines labeled with the total LS , $L'S'$ momenta of the left-hand and right-hand states respectively, i.e., the coupling of L and S to resultant J is ignored at this point.

(v) Contract the two state graphs with the interaction graph by joining corresponding lines representing interacting electrons or groups of spectator electrons.

(vi) For each subshell in the left-hand and right-

hand states containing one or more interacting electrons, multiply the diagram resulting from step (v) by the appropriate c.f.p. and sum over all alternative parentage.

(vii) Replace the cross on each Coulomb line in the result of step (vi) by the appropriate factor $(-1)^k X(k; \lambda \mu \lambda' \mu')$. Sum over all k . Where an open k line representing a multipole operator occurs, remove the double bar and multiply the result of step (vi) by the factor $I(k; \lambda \lambda')$.

(viii) Multiply the result of step (vii) by a weight factor $[N_\lambda! / (N_\lambda - n_\lambda)!]^{1/2}$ for each interacting subshell in the left-hand state and a factor $[N_{\lambda'}! / (N_{\lambda'} - n_{\lambda'})!]^{1/2}$ for each interacting subshell in the right-hand state. Here $n_\lambda n_{\lambda'}$ are the numbers of interacting electrons in subshell λ on the left-hand side and right-hand side, respectively.

For a one-electron operator graph, the weight factor is $(N_\rho N_{\rho'})^{1/2}$. For a two-electron operator graph the factor is

$$[N_\rho(N_\sigma - \delta(\rho\sigma))N_{\rho'}(N_{\sigma'} - \delta(\rho'\sigma'))]^{1/2}. \quad (6.3)$$

For a single Coulomb interaction graph which has $\rho = \sigma$, $\rho' = \sigma'$ the factor (6.3) is multiplied by an additional factor $\frac{1}{2}$ in accordance with the condition $i < j$ in (3.19).

(ix) Multiply the result of step (viii) by the Pauli phase factor $(-1)^{P_A - P_B}$ where

$$P_{A,B} = \sum_\nu \sum_{\lambda=\nu+1}^{\infty} \bar{N}_\lambda,$$

and the summation ν runs over the interacting subshells in the configurations A and B , respectively. For a two-electron operator with interacting subshells ρ , σ on the left and $\rho'\sigma'$ on the right, the exponent can be written (F65)

$$P_A - P_B = \sum_{\lambda=\rho+1}^{\sigma} \bar{N}_\lambda - \sum_{\lambda=\rho'+1}^{\sigma'} \bar{N}_\lambda.$$

(x) If the diagram resulting from step (vii) does *not* contain a free k interaction line, join the total LS angular momentum line of the left-hand state with the total $L'S'$ angular momentum line of the right-hand state and multiply by a factor $[L]^{-1}[S]^{-1}\delta(LL')\delta(SS')$, as given by Eq. (4.3). If a free k line does occur, join the LS and $L'S'$ lines with the k line to form a node in which the lines have the cyclic order $L'kL$ and multiply by the factor $[S]^{-1}\delta(SS')$ in accordance with the results of Sec. 5.2. The orientation of this node is opposite to that specified in Sec. 5.2. This reversal is necessary since step (iv) of Sec. 4.2 is omitted for the orbital diagram.

(xi) Reduce the diagram to a product or sum of products of 6- j coefficients by applying steps (i)-(v) of Sec. 4.2 and the methods of Sec. 4.3.

Step (xi) completes the evaluation of the matrix

element of one n -electron interaction graph. Steps (iii)–(xi) are then repeated for all other interaction graphs contributing to the matrix element and the partial results added. There remains the additional step.

(xii) For the matrix element involving a multipole operator between a state on the left with total quantum numbers $LSJM$ and a state on the right with total quantum numbers $L'S'J'M'$, multiply by a factor

$$(-1)^{L+S-M} ([J][J'])^{1/2} \delta(SS') \times \begin{pmatrix} J' & k & J \\ M' & q & -M \end{pmatrix} \begin{Bmatrix} k & J & J' \\ S & L' & L \end{Bmatrix},$$

which was derived in Sec. 5.2.

6.2 Example

The step-by-step procedure of Sec. 6.1 will be applied to a particular example of a Coulomb matrix element. We will consider the matrix element

$$M = ((\pi^{N_\pi} L_\pi S_\pi, (\rho\sigma) \hat{L} \hat{S}), LS | \sum_{i < j} V_{ij} | \times (\pi^{N_\pi - 1} \bar{L}_\pi \bar{S}_\pi, \rho^2 L_\rho S_\rho) \hat{L}' \hat{S}', \tau, LS), \quad (6.5)$$

where $N_\pi = (4l_\pi + 2)$, i.e., the π subshell is closed on the left. Also, we assume that all subshells which precede subshell π are closed and therefore can be ignored. An example of a matrix element of this type is that considered by Armstrong (A68), i.e.,

$$M = (5d^{10} 1S, (5s6p), {}^{2S+1}P | \sum_{i < j} V_{ij} | 5d^9 \times {}^2D, 5s^2 1S, 7p, {}^{2S+1}P). \quad (6.6)$$

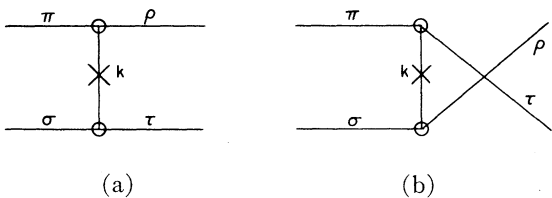
Step (i). The configurations differ in the quantum numbers of just two electrons so that there is a unique choice of interacting subshells. These subshells are π, σ on the left and ρ, τ on the right.

The corresponding configuration of the spectator electrons is

$$\bar{N}_\pi = N_\pi - 1, \quad \bar{N}_\rho = 1, \quad \bar{N}_\sigma = 0, \quad \bar{N}_\tau = 0,$$

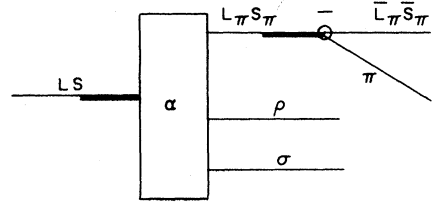
which gives $\sum_\lambda \bar{N}_\lambda = N_\pi$ in accordance with (6.2).

Step (ii). The interaction graphs are



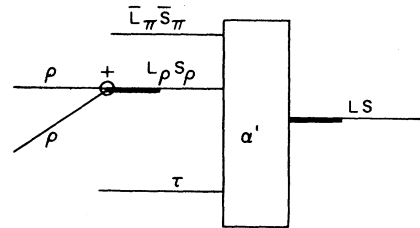
(6.7)

Step (iii). Graph (a) has a phase +1 and graph (b) has a phase (-1). We will consider graph (a) first. *Step (iv).* The state graphs are



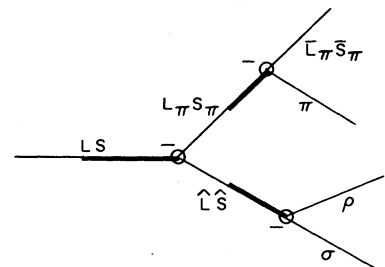
(6.8)

for the left-hand state, and



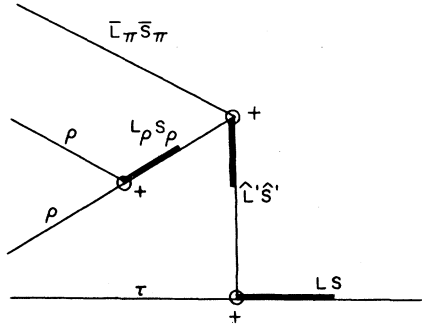
(6.9)

for the right-hand state. In this example, graph (6.8) stands for the coupling scheme



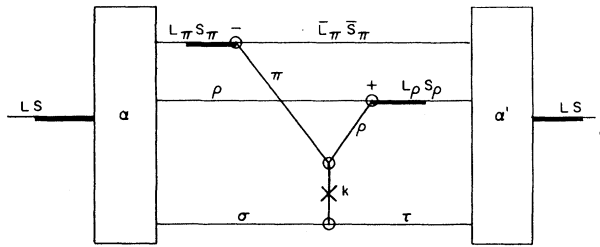
(6.10)

and graph (6.9) stands for the coupling scheme



(6.11)

Step (v). Contraction of (6.7)-(6.9) gives the diagram



(6.12)

Step (vi). All the c.f.p. are trivially unity. In particular, for the ρ shell we have the condition

$$\begin{aligned} (\rho | \rho^2 L_\rho S_\rho) &= 1 & L_\rho + S_\rho \text{ even} \\ &= 0 & L_\rho + S_\rho \text{ odd.} \end{aligned} \quad (6.13)$$

Step (vii). Remove the cross on the k line and multiply the diagram (6.12) by $(-1)^k X(k; \pi \sigma \rho \tau)$. Sum over all k .

Step (viii). The weight factor is

$$(N_\pi \times 2)^{1/2} = 2[L_\pi]^{1/2}. \quad (6.14)$$

Step (ix). The Pauli phase factor is -1 , since $P_A = 1, P_B = 0$.

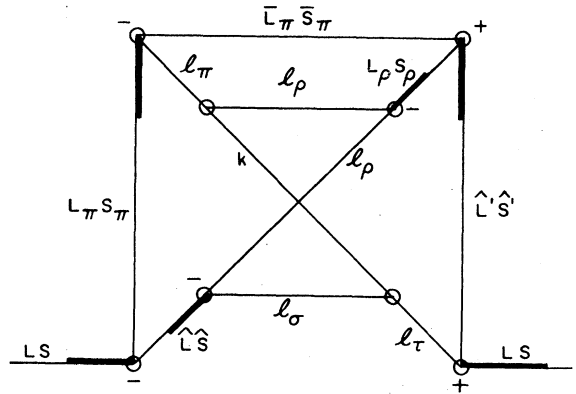
The matrix element of the part of the Coulomb interaction represented by graph (a) has now been

obtained in the form

$$\bar{M}_a(\pi\sigma, \rho\tau) = -2[l_\pi]^{1/2} \sum_k (-1)^k X(k; \pi\sigma, \rho\tau) \times \mathcal{G}, \quad (6.15)$$

where

$\mathcal{G} =$



(6.16)

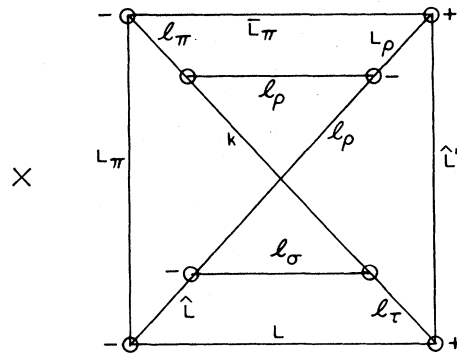
The diagram \mathcal{G} is obtained from (6.12) by specifying the coupling schemes as in (6.10) and (6.11). The $(l_\rho l_\rho) L_\rho S_\rho$ node has a minus sign to compensate for the change of its orientation with respect to diagram (6.11).

Steps (x) and (xi). Contracting the LS lines in (6.16) and application of steps (i)-(v) of Sec. 4.2 give

$$\mathcal{G} = \mathcal{L} \times \mathcal{S},$$

where

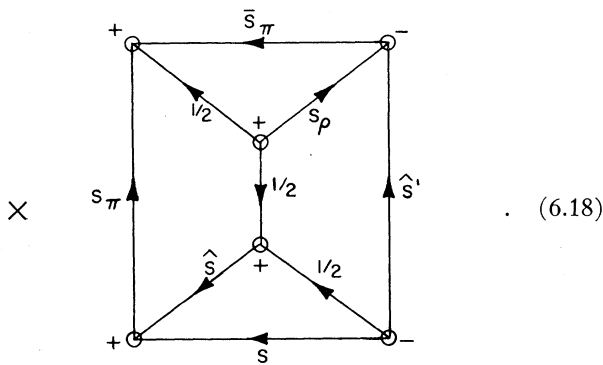
$$\mathcal{L} = ([L_\pi][\hat{L}][L_\rho][\hat{L}'])^{1/2}$$



(6.17)

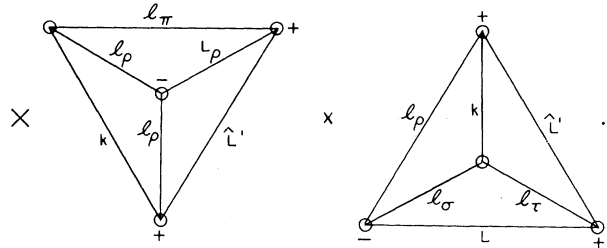
and

$$s = ([S_\pi][\hat{S}][S_\rho][\hat{S}'])^{1/2}$$



k, l_ρ, \hat{L}' to give

$$\mathcal{L} = [l_\pi]^{-1/2} ([L_\rho][\hat{L}'])^{1/2} \delta(l_\pi \bar{L}_\pi) \delta(\hat{L}L)$$



(6.18)

(6.20)

Comparison of each diagram with (4.20) gives the result

$$\mathcal{L} = [l_\pi]^{-1/2} ([L_\rho][\hat{L}'])^{1/2} \delta(l_\pi \bar{L}_\pi) \delta(\hat{L}L)$$

$$\times (-1)^{l_\rho + L_\rho + l_\sigma + L} \begin{Bmatrix} L_\rho & l_\rho & l_\rho \\ k & \hat{L}' & l_\pi \end{Bmatrix} \times \begin{Bmatrix} k & l_\sigma & l_\tau \\ L & \hat{L}' & l_\rho \end{Bmatrix}$$

(6.21)

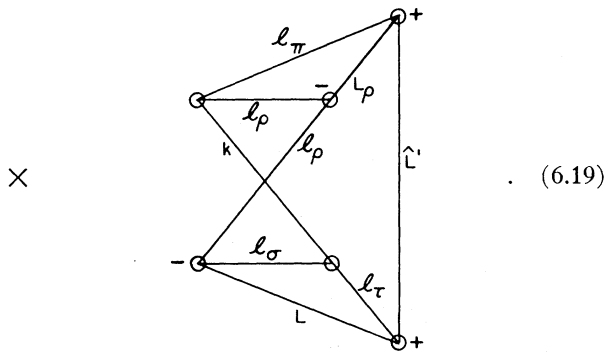
The diagrams in (6.17) and (6.18) are evaluated by the procedure of Sec. 4.3 as follows.

(a) The orbital diagram. Since π is a closed subshell, then $L_\pi = 0$. Removal of the L_π line gives the result

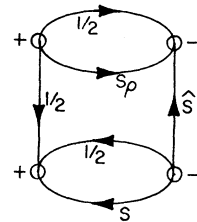
$$\mathcal{L} = [l_\pi]^{-1/2} ([L_\rho][\hat{L}'])^{1/2} \delta(l_\pi \bar{L}_\pi) \delta(\hat{L}L)$$

(b) The spin diagram. Removal of the S_π line gives

$$s = 2^{-1/2} ([S_\rho][\hat{S}'])^{1/2} \delta(\bar{S}_{\pi\frac{1}{2}}) \delta(S\hat{S})$$



(6.19)



(6.22)

Removal of one closed loop gives the unit diagram (4.18) and the final result.

$$s = [S_\rho]^{1/2} / 2 \delta(\bar{S}_{\pi\frac{1}{2}}) \delta(S\hat{S}) \delta(\bar{S}_{\rho\frac{1}{2}}) \Delta(S_{\frac{1}{2}\frac{1}{2}}). \quad (6.23)$$

The diagram in (6.19) separates on the three lines

By substitution of the results (6.21) and (6.23) into

Eq. (6.15) we obtain

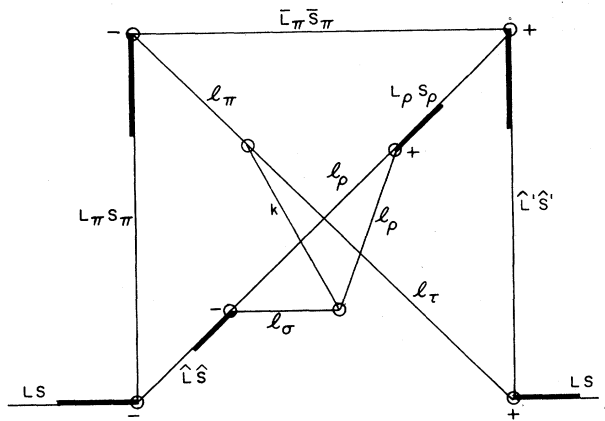
$$\begin{aligned} \bar{M}_a(\pi\sigma, \rho\tau) &= -([\hat{L}'] [L_\rho] [S_\rho])^{1/2} \\ &\times (-1)^{l_\rho + L_\rho + l_\sigma + L} \sum_k \begin{Bmatrix} L_\rho & l_\rho & l_\rho \\ k & \hat{L}' & l_\pi \end{Bmatrix} \begin{Bmatrix} k & l_\sigma & l_\tau \\ L & \hat{L}' & l_\rho \end{Bmatrix} \\ &\times (-1)^k X(k; \pi\sigma\rho\tau). \end{aligned} \quad (6.24)$$

We now consider the contribution of graph (b) of step (ii) to the matrix element. Step (iii) gives a phase factor (-1) . Steps (iv)–(ix) yield exactly the same factors as for graph (a) since these factors depend only upon which subshells are concerned in the interaction. From step (ix) we have the result

$$\bar{M}_b(\pi\sigma, \rho\tau) = 2[l_\pi]^{1/2} \sum_k (-1)^k X(k; \pi\sigma\tau\rho) g, \quad (6.25)$$

where

$g =$



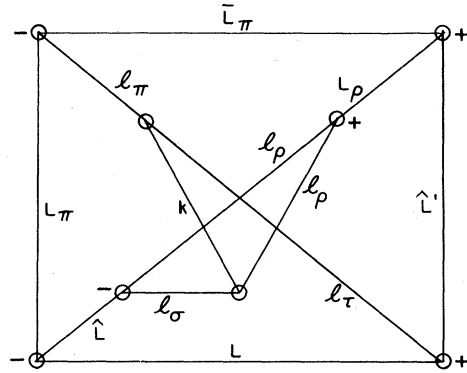
(6.26)

Steps (x) and (xi). Application of steps (i)–(iv) of Sec. 4.2 gives the product

$$g = \mathcal{L} \times s$$

where

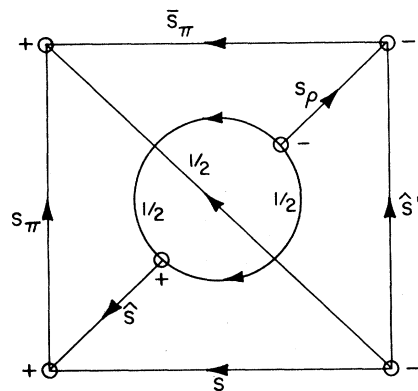
$$\mathcal{L} = ([L_\pi] [\hat{L}] [L_\rho] [\hat{L}'])^{1/2} \times$$



(6.27)

and

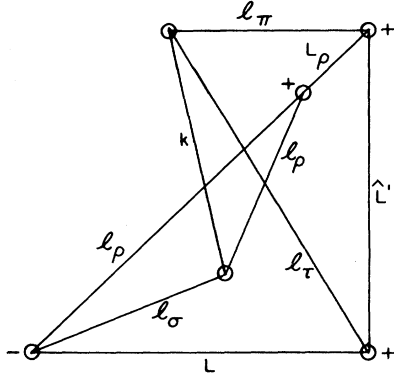
$$s = ([S_\pi] [\hat{S}] [S_\rho] [\hat{S}'])^{1/2} \times$$



(6.28)

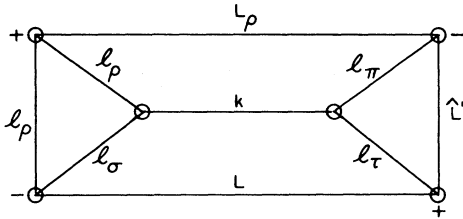
The orbital diagram is evaluated by first removing

the L_π line (since $L_\pi=0$) to give
 $\mathcal{E} = [l_\pi]^{-1/2} ([L_\rho][\hat{L}'])^{1/2} \delta(l_\pi \bar{L}_\pi) \delta(\hat{L}L)$.



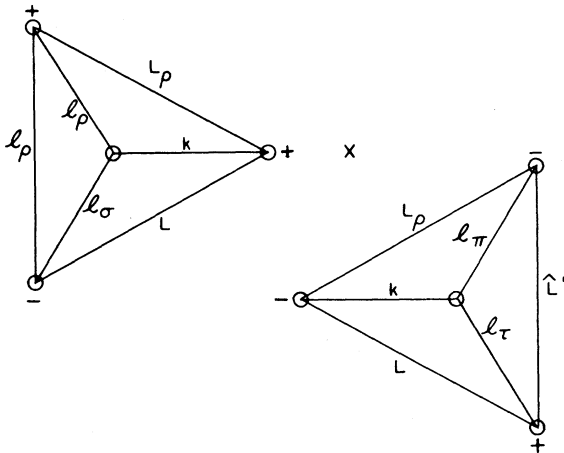
(6.29)

The diagram in (6.29) can be deformed into



Separation on the lines L_ρ , L , and k gives

$$\mathcal{E} = [l_\pi]^{-1/2} ([L_\rho][\hat{L}'])^{1/2} \delta(l_\pi \bar{L}_\pi) \delta(\hat{L}L)$$



(6.30)

$$= [l_\pi]^{-1/2} ([L_\rho][\hat{L}'])^{1/2} \delta(l_\pi \bar{L}_\pi) \delta(\hat{L}L) \times (-1)^{\hat{L}'+l_\pi} \begin{Bmatrix} k & L & L_\rho \\ l_\rho & l_\rho & l_\sigma \end{Bmatrix} \times \begin{Bmatrix} k & L_\rho & L \\ \hat{L}' & l_\tau & l_\pi \end{Bmatrix}$$

Removal of the S_π line in the spin diagram gives

$$s = 2^{-1/2} ([S_\rho][\hat{S}'])^{1/2} \delta(S\hat{S}) \delta(S_\pi \frac{1}{2}) \times 1/2 \cdot (6.31)$$

Removal of one closed loop reduces the diagram in (6.31) to the unit diagram (4.18), so that

$$s = (2[S_\rho])^{-1/2} [\hat{S}']^{1/2} \delta(S\hat{S}) \delta(\bar{S}_\pi \frac{1}{2}) \delta(S_\rho S) \Delta(\frac{1}{2} \frac{1}{2} S) \cdot (6.32)$$

By substitution of the results (6.32) and (6.30) in Eq. (6.25) we obtain the final result

$$\bar{M}_b(\pi\sigma, \rho\tau) = (2[L_\rho][\hat{L}'][\hat{S}'])^{1/2} \times [S_\rho]^{-1/2} \delta(SS_\rho) \sum_k (-1)^{\hat{L}'+l_\pi+k} X(k; \pi\sigma\tau\rho) \times \begin{Bmatrix} k & L & L_\rho \\ l_\rho & l_\rho & l_\sigma \end{Bmatrix} \begin{Bmatrix} k & L_\rho & L \\ \hat{L}' & l_\tau & l_\pi \end{Bmatrix} \cdot (6.33)$$

In the example (6.6), we have $\hat{L}'=2$ and $\hat{S}'=\frac{1}{2}$, i.e., a $2D$ state. Substituting the appropriate numerical values in (6.24), we find, since $k=2$ only,

$$\bar{M}_a(\pi\sigma, \rho\tau) = -5^{1/2} \begin{Bmatrix} 0 & 0 & 0 \\ 2 & 2 & 2 \end{Bmatrix} \begin{Bmatrix} 2 & 1 & 1 \\ 1 & 2 & 0 \end{Bmatrix} \times X(2; 5d6p5s7p) = -1/(15)^{1/2} X(2; 5d6p5s7p) = \sqrt{2}/5 R^2(5d6p5s7p) \cdot (6.34)$$

Similarly for (6.33) we have $k=1$ only and

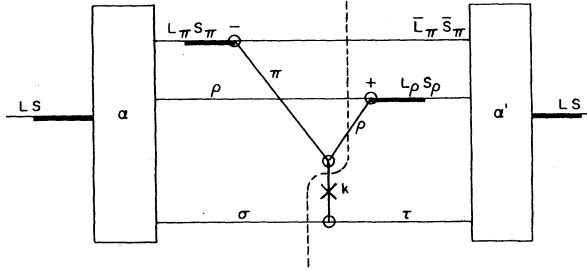
$$\bar{M}_b(\pi\sigma, \rho\tau) = -(2 \times 5 \times 2)^{1/2} \delta(S0) X(1; 5d6p7p5s) \times \begin{Bmatrix} 1 & 1 & 0 \\ 0 & 0 & 1 \end{Bmatrix} \times \begin{Bmatrix} 1 & 0 & 1 \\ 2 & 1 & 2 \end{Bmatrix} = -2/3 \delta(S0) X(1; 5d6p7p5s) = -2\sqrt{2}/3 \delta(S0) R^1(5d6p7p5s) \cdot (6.35)$$

The results (6.34) and (6.35) have been given previously by Armstrong (A68).⁵

As mentioned at the beginning of Sec. 4, an alternative to the graphical evaluation of the \mathcal{G} diagram [step (xi)] is to derive the corresponding recoupling

⁵ Armstrong uses the spherical harmonics of FR59, Eq. (5.17) to define the Racah tensors $C^{[k]}$ and the one-electron angular momentum eigenstates. Hence, to agree with our result (6.34) and (6.35) one must substitute in the result of step (f) of A68 the $(l||C^{[k]}||l')$ of FR59 Eq. (14.12) and multiply by $(-1)^{1/2(-l_a-l_b+l_c+l_d)}$, where a, b are the interacting subshells in the left-hand wave function and c, d are those in the right-hand wave function. See also Footnote 1.

coefficient which is then evaluated using Burke's computer program. The recoupling coefficient is obtained by separating the \mathcal{G} diagram into two parts by an imaginary line which bisects the k line and each line representing spectator electrons. The two parts of the separated diagram represent the lhs and rhs of the recoupling coefficient. The free lines represent the momenta which are coupled according to the schemes α and α' of the lhs and rhs, respectively. For example, the \mathcal{G} diagram (6.12) is separated as follows:



and corresponds to the recoupling coefficient

$$\mathcal{G} = ([l_\pi][l_\tau])^{-1/2} ([\bar{L}_\pi \bar{S}_\pi, (l_\rho^{(2)} k) l_\pi] L_\pi S_\pi, l_\rho^{(1)}, l_\sigma, \alpha | \bar{L}_\pi \bar{S}_\pi, (l_\rho^{(1)} l_\rho^{(2)}) L_\rho S_\rho, (k l_\sigma) l_\tau, \alpha')^{(L, S)}. \quad (6.36)$$

The factor $([l_\pi][l_\tau])^{-1/2}$ appears since the "thick-labeling" of the lines π and τ in (6.7) was omitted in Sec. 2. In the recoupling coefficient it is necessary to distinguish the two electrons which carry orbital momentum l_ρ . The coefficient (6.36) separates into a product of spin and orbital coefficients

$$\mathcal{L} = ([l_\pi][l_\tau])^{-1/2} ([\bar{L}_\pi (l_\rho^{(2)} k) l_\pi] L_\pi, l_\rho^{(1)}, l_\sigma, \alpha | \bar{L}_\pi, (l_\rho^{(1)} l_\rho^{(2)}) L_\rho, (k l_\sigma) l_\tau, \alpha')^{(L)} \quad (6.37)$$

and

$$\mathcal{S} = ((\bar{S}_\pi, s_\rho^{(2)}) S_\pi, s_\rho^{(1)}, s_\sigma, \alpha | \bar{S}_\pi (s_\rho^{(1)} s_\rho^{(2)}) S_\rho, s_\sigma, \alpha')^{(S)}, \quad (6.38)$$

where $s_\rho = s_\sigma = \frac{1}{2}$. The recoupling coefficients (6.37) and (6.38) are those obtained by the orbiton method of Fano (F65). The above procedure of bisecting the k line and associating one vertex of the interaction graph with the lh state graph and the other with the rh state graph corresponds to the "emission" and "absorption" of an orbiton in Fano's method.

The coefficients (6.37) and (6.38) can be evaluated by use of the computer program given in B70 or by a direct expansion as used in FR59. Finally, it is immaterial which vertex of the interaction graph is associated

with which side of the recoupling coefficient. For example, we can separate the diagram (6.12) by a line which bisects the lines π and τ rather than the lines ρ and σ as was done above. This procedure leads to the recoupling coefficient

$$\mathcal{G} = [l_\rho]^{-1/2} [l_\sigma]^{-1/2} ((\bar{L}_\pi \bar{S}_\pi, l_\pi) L_\pi S_\pi, l_\rho^{(1)}, (k l_\tau) l_\sigma, \alpha | \bar{L}_\pi \bar{S}_\pi, [l_\rho^{(1)}, (l_\pi k) l_\rho^{(2)}] L_\rho S_\rho, l_\tau, \alpha')^{(L, S)},$$

which may be shown to be equal to (6.36).

7. SUMS OF PRODUCTS OF MATRIX ELEMENTS

Thus far we have considered the matrix elements of a single Coulomb or multipole interaction operator between states of the same or different configurations. In the perturbation theory of configuration interaction there has arisen the need to evaluate sums of products of matrix elements between states of different configurations (RW63, RS67, W68). For example (W68), the interaction $(A\alpha | \sum_{i<j} V_{ij} | A\alpha')$ between the states α, α' of a particular configuration A is subject to a second-order correction,

$$P = (1/\Delta E_{AB}) \sum_{\beta} (A\alpha | \sum_{i<j} V_{ij} | B\beta) (B\beta | \sum_{r<s} V_{rs} | A\alpha') \quad (7.1)$$

due to interaction with the states β of another configuration B . In this expression, ΔE_{AB} is the difference between the zero-order energies of configurations A and B .

Perturbation terms of the type (7.1) were first studied in detail by Rajnak and Wybourne (RW63), where it was shown that the second-order perturbation sum can be replaced by the matrix element of an *effective* operator acting within the configuration A . The analysis of RW63 was subsequently refined by Racah and Stein (RS67) by the introduction of "curtailed" operators (see Sec. 3) and Wybourne (W68) has since given a comprehensive discussion of the application of this method. The primary aim of this work has been to derive and to investigate the *structure* of the effective operators. In the following, the emphasis will be on the explicit numerical evaluation of the perturbation terms. The graphical representation of the curtailed operators of RS67 introduced in Sec. 3 will be used. As has been demonstrated by Judd (J67) and Sandars (S69) the graphical representation is also very convenient for the study of the structure of the effective operators.

We will restrict the detailed discussion to second-order terms of the type (7.1) but the extension to higher-order-perturbation terms can be made in an obvious way. The modification necessary when a multipole interaction matrix element is substituted for one of the Coulomb matrix elements will be indicated.

7.1 Effective Operators

In Sec. 3 it was shown that the matrix element of the Coulomb operator $\sum_{i<j} V_{ij}$ can be replaced by the equivalent matrix element of the curtailed operator \bar{V} where

$$\bar{V} = \sum_{\{\lambda\mu, \lambda'\mu'\}} \bar{V}(\lambda\mu, \lambda'\mu') \quad (7.2)$$

and $\bar{V}(\lambda\mu, \lambda'\mu')$ is one of the operators (3.12), (3.16), or (3.19). The summation in (7.2) runs over the sets $\{\lambda\mu, \lambda'\mu'\}$ of interacting subshells which contribute to the Coulomb matrix element between the configurations A and B . In this way the perturbation term P may be written

$$P = (1/\Delta E_{AB}) \sum_{\beta} (A\alpha | \sum_{\{\lambda\mu, \lambda'\mu'\}} \bar{V}(\lambda\mu, \lambda'\mu') | B\beta) \times (B\beta | \sum_{\{\nu\pi, \nu'\pi'\}} \bar{V}(\nu\pi, \nu'\pi') | A\alpha'). \quad (7.3)$$

Since the curtailed operators connect configuration A only with configuration B , the summation over states β can be formally extended over the states of all other configurations of the N electrons. Furthermore, since we will deal with symmetric operators which connect the antisymmetric states $(A\alpha |$ only with other antisymmetric states, the sum may be extended over states of all symmetries. In this way the sum over states in (7.3) can be extended formally over the complete set of states of the N -electron system, so that by closure we have

$$P = (1/\Delta E_{AB}) \times (A\alpha | \sum_{\{\lambda\mu, \lambda'\mu'\}} \sum_{\{\nu\pi, \nu'\pi'\}} \bar{V}(\lambda\mu, \lambda'\mu') \bar{V}(\nu\pi, \nu'\pi') | A\alpha'). \quad (7.4)$$

The perturbation sum has now been replaced by the matrix element of an *effective* operator. As in (3.21) for the single Coulomb operator, the matrix element in (7.4) can be written as a sum of contributions from different sets of interacting subshells, i.e.,

$$P = (1/\Delta E_{AB}) \sum_{\{\lambda\mu, \lambda'\mu'\}} \sum_{\{\nu\pi, \nu'\pi'\}} \bar{P}(\lambda\mu\lambda'\mu'; \nu\pi\nu'\pi'), \quad (7.5a)$$

where

$$\bar{P}(\lambda\mu\lambda'\mu'; \nu\pi\nu'\pi') = (A\alpha | \bar{V}(\lambda\mu, \lambda'\mu') \bar{V}(\nu\pi, \nu'\pi') | A\alpha'). \quad (7.5b)$$

We will consider the evaluation of the matrix element $\bar{P}(\lambda\mu\lambda'\mu'; \nu\pi\nu'\pi')$. First we will obtain a graphical representation of the product operator $\bar{V}(\lambda\mu, \lambda'\mu') \bar{V}(\nu\pi, \nu'\pi')$ from the representation (3.12), (3.16), or (3.19) of each operator \bar{V} . The matrix element (7.5b) is then evaluated by bracketing the graphical representation of the product operator with the graphical representations [of the form (2.15)] of the states $(A\alpha |$ and $|A\alpha')$. The procedure is the same as was used in Sec. 3 for the

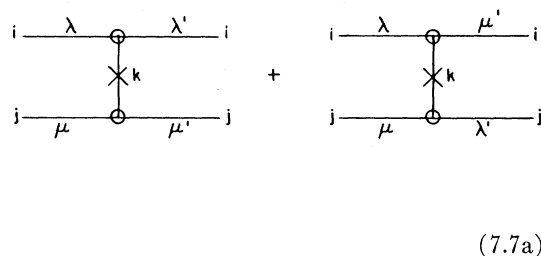
matrix element of the single Coulomb operator (2.9). However, each Coulomb operator \bar{V} is a two-electron operator so that, as we shall see, the product operator can be expressed as a sum of four-, three-, and two-electron operators. Each n -electron operator gives rise to a different weight factor and Pauli phase factor. The remainder of Sec. 7.1 will be mainly concerned with the evaluation of these factors.

For greatest generality we will assume that in the product $\bar{V}(\lambda\mu, \lambda'\mu') \bar{V}(\nu\pi, \nu'\pi')$, we have the conditions

$$\lambda \neq \mu, \quad \lambda' \neq \mu', \quad \nu \neq \pi, \quad \nu' \neq \pi'. \quad (7.6)$$

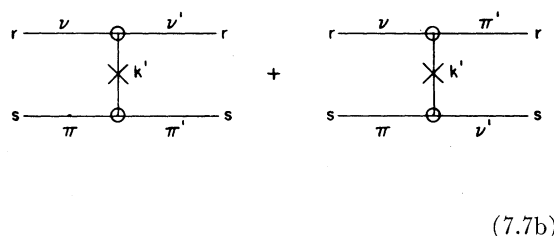
Consequently we use the form (3.12) of the curtailed operators, i.e.,

$$\bar{V}(\lambda\mu, \lambda'\mu') = \sum_{i \neq j} \sum_k$$



and

$$\bar{V}(\nu\pi, \nu'\pi') = \sum_{r \neq s} \sum_{k'}$$



In general the operators (7.7a) and (7.7b) do not commute.

In the product of the operators (7.7a) and (7.7b) there are various classes of terms which are characterized by the number of electrons involved in the effective interaction. The enumeration of the four-, three-, and two-electron operator graphs corresponds to writing down all the Feynman graphs which contribute to the second-order interaction as is done in Chapter 4 of Judd (J67), for example. The operator (7.7b) transfers the pair of electrons r, s out of the subshells ν', π' into the subshells ν, π and the operator (7.7a) transfers the pair of electrons i, j out of the subshells λ', μ' into the subshells λ, μ . The various n -electron

graphs in the product of these operators are obtained as follows:

(1) If the subshells λ', μ' are both distinct from the subshells ν, π , then clearly *only* terms with $i \neq j \neq r \neq s$ are allowed in the product of (7.7a) and (7.7b). For example, the product of the first graph of (7.7a) with the first graph of (7.7b) gives the four-electron operator

$$\sum_{i \neq j \neq r \neq s} \sum_{kk'} \begin{array}{c} i \text{---} \lambda \text{---} \bigcirc \text{---} \lambda' \text{---} i \\ | \\ \times^k \\ | \\ j \text{---} \mu \text{---} \bigcirc \text{---} \mu' \text{---} j \\ \\ r \text{---} \nu \text{---} \bigcirc \text{---} \nu' \text{---} r \\ | \\ \times^{k'} \\ | \\ s \text{---} \pi \text{---} \bigcirc \text{---} \pi' \text{---} s \end{array} \quad (7.8)$$

(2) If either of λ' or μ' is the same subshell as either of ν or π , then it is possible that one of the electrons shifted by the operator (7.7b) will be shifted again by the operator (7.7a). In other words, only three electrons take part in the interaction. Therefore, in addition to the four-electron terms of the type (7.8), in this case the product of (7.7a) and (7.7b) contains three-electron terms. These three-electron operator graphs are obtained by contracting a line on the right of the graphs (7.7a) with a one-electron line carrying the *same* electron *and* subshell labels on the left of the graphs of (7.7b). For example, if $\mu' = \nu$ and $\lambda' \neq \pi$, the product of (7.7a) and (7.7b) contains four three-electron graphs. The first is obtained by putting $j = r$ in the product of the first graph of (7.7a) and the first graph of (7.7b) and contracting the corresponding lines, i.e.,

$$\sum_{i \neq j \neq s} \sum_{kk'} \begin{array}{c} i \text{---} \lambda \text{---} \bigcirc \text{---} \lambda' \text{---} i \\ | \\ \times^k \\ | \\ j \text{---} \mu \text{---} \bigcirc \text{---} \mu' \text{---} j \\ | \\ \times^{k'} \\ | \\ s \text{---} \pi \text{---} \bigcirc \text{---} \pi' \text{---} s \end{array} \quad (7.9)$$

(3) If the pair of subshells λ', μ' is identical to the pair of subshells ν, π , then the pair of electrons shifted by the operator (7.7b) may be shifted again by (7.7a). In this case there will be four-, three-, and two-electron terms in the product of (7.7a) and (7.7b). The two-electron operator graphs are obtained by contracting *two* open lines on the right of the graphs (7.7a) with two open lines on the left of the graphs (7.7b). For example, if $\lambda' = \nu$ and $\mu' = \pi$, the product of the first graph in (7.7a) with the first graph in (7.7b) contains terms with $i = r, j = s$, i.e.,

$$\sum_{i \neq j} \sum_{kk'} \begin{array}{c} i \text{---} \lambda \text{---} \bigcirc \text{---} \lambda' \text{---} \bigcirc \text{---} \nu' \text{---} i \\ | \quad | \\ \times^k \quad \times^{k'} \\ | \quad | \\ j \text{---} \mu \text{---} \bigcirc \text{---} \mu' \text{---} \bigcirc \text{---} \pi' \text{---} j \end{array} \quad (7.10)$$

All graphs formed from the product of (7.7a) and (7.7b) do not necessarily give a nonzero contribution to the term $\bar{P}(\lambda\mu\lambda'\mu'; \nu\pi\nu'\pi')$. This follows from the orthonormality of one-electron wave function which corresponds to the requirement that two lines representing the same electron give a nonzero contraction only if they carry the same subshell label. Clearly, for each subshell λ , the number of lines entering and leaving each operator graph must not exceed the occupation number of subshell λ in the left-hand and right-hand states, respectively.

The first step in the evaluation of the matrix element $\bar{P}(\lambda\mu, \lambda'\mu'; \nu\pi\nu'\pi')$ of the operator $\bar{V}(\lambda\mu, \lambda'\mu')\bar{V}(\nu\pi, \nu'\pi')$ is to enumerate the various four-, three-, and two-electron terms in the product of (7.7a) and (7.7b) according to the conditions (1), (2), and (3) above. The contribution of each n -electron term is then obtained by contracting each operator graph with the graph of the wave functions of the states $|A\alpha\rangle$ and $|A\alpha'\rangle$.

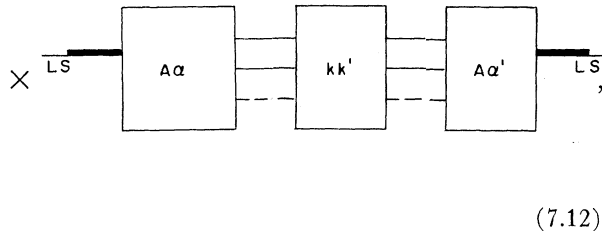
In each n -electron interaction graph of the form (7.8), (7.9), or (7.10) the interacting electrons i, j, \dots , etc. may be labeled $(N-n+1), (N-n+2) \dots N$ and the sum over $i \neq j \neq \dots$ replaced by the factor $N(N-1) \dots (N-n+1)$. The graphs of the wave functions of $|A\alpha\rangle$ and $|A\alpha'\rangle$ are of the form (2.15) and (2.16) with the n interacting electrons separated by fractional parentage expansions like (2.18) or (2.19). We shall consider the matrix element, $\bar{P}_n^m(\lambda\mu\lambda'\mu'; \nu\pi\nu'\pi')$ of one n -electron operator graph, say the m th, in the product $\bar{V}(\lambda\mu, \lambda'\mu')\bar{V}(\nu\pi, \nu'\pi')$, i.e., in the product of (7.7a) and (7.7b). As in Sec. 3.1

for the two-electron single Coulomb matrix elements, the matrix element of each n -electron operator graph must be diagonal in the distributions \bar{q}, \bar{q}' of the $(N-n)$ spectator electrons. We need consider only one such diagonal distribution and multiply by the number [see Eq. (3.4)]

$$\bar{\mathfrak{U}} = (N-n)! / (\prod_{\lambda} N_{\lambda}!) \quad (7.11)$$

of such distributions. The distribution of the interacting electrons amongst the subshells in $(A\alpha |$ and $| A\alpha')$ is fixed by their distribution on the left and right, respectively, of the operator graph. The operator graph is then drawn with the open lines ordered vertically downwards according to the order of the subshell with which each line is labeled. Integration over all electron coordinates is performed symbolically by bracketing the n -electron operator graph with the wave function graphs and contracting corresponding free lines. This procedure, which is the same as led from (2.15), (2.16), and (3.6) to (3.7), gives the matrix element $\bar{P}_n^m(\lambda\mu\lambda'\mu'; \nu\pi\nu'\pi')$ in the form

$$\bar{P}_n^m(\lambda\mu\lambda'\mu'; \nu\pi\nu'\pi') = (-1)^{P_A+P_{A'}+P_{int}} F_n^m \sum_{kk'} \sum_{f.p.}$$



(7.12)

where the central block, labeled kk' , represents the n -electron interaction graph. The weight factor F_n^m , for any n -electron graph of the form (7.8), (7.9), or (7.10) is given by, from (2.15), (2.16), and (7.11),

$$F_n^m = [(N-n+1) \cdots N] (\mathfrak{U}\bar{\mathfrak{U}}')^{-1/2} \bar{\mathfrak{U}} \\ = [\prod_{\lambda} N_{\lambda}! / (N_{\lambda} - n_{\lambda})!]^{1/2} [\prod_{\lambda} N_{\lambda}'! / (N_{\lambda}' - n_{\lambda}')!]^{1/2}, \quad (7.13)$$

where $n_{\lambda}, n_{\lambda}'$ are the numbers of interacting electrons in subshell λ in the left-hand and right-hand configurations, respectively. The factor (7.13) has already been given in step (viii) of Sec. 6.1 with reference to the two-electron interaction graph. Similarly, the Pauli phase factor is given in step (ix) of Sec. 6.1 by

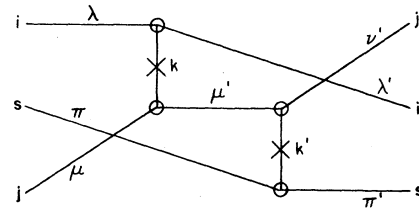
$$P_A = \sum_{\nu} \sum_{\lambda=\nu+1}^{\infty} \bar{N}_{\lambda}, \quad P_{A'} = \sum_{\nu'} \sum_{\lambda=\nu'+1}^{\infty} \bar{N}_{\lambda},$$

where the summation ν is over the interacting subshells in the left-hand state $(A\alpha |$ and the summation ν' over those in the right-hand state $| A\alpha')$.

The Pauli phase factor $(-1)^{P_{int}}$ in (7.12) comes from the permutation of the interacting electrons

themselves [see Sec. 3.2]. As in the case of two-electron operators, this factor is obtained by drawing the n -electron interaction graph with the free lines ordered vertically downwards according to the ordering of the subshells. Then P_{int} is equal to the number of times that one-electron lines cross. For example, if in the three-electron interaction (7.9) we have the order $\lambda < \pi < \mu$ on the left and the order $\nu' < \lambda' < \pi'$ on the right, then the graph is drawn

$$\sum_{i \neq j \neq s} \sum_{kk'}$$



(7.14)

In the matrix element of (7.14), the lines $i, j,$ and s are labeled $N-2, N-1,$ and $N,$ respectively, and the summation over i, j, s replaced by the factor $N(N-1)(N-2)$. Each crossing of one-electron lines then represents a single permutation of the electrons $N-2, N-1, N$ from their standard order. Hence, in this example, P_{int} in Eq. (7.12) is equal to 2. The evaluation of the matrix element $P_n^m(\lambda\mu\lambda'\mu'; \nu\pi\nu'\pi')$ proceeds by replacing the crosses on the interaction lines in the central block of the diagram in (7.12) by the corresponding factors of the type $(-1)^k X(k; \lambda\mu\lambda'\mu')$. For each subshell containing interacting electrons the full squares on certain nodes arising from f.p. expansions like (2.18) or (2.19) are replaced by the corresponding c.f.p. The remaining diagram in (7.12) is a \mathfrak{g} diagram and is evaluated by the method of Sec. 4.

The matrix element $\bar{P}(\lambda\mu\lambda'\mu'; \nu\pi\nu'\pi')$ is then obtained by repeating the above procedure to obtain the matrix elements of all two-, three-, and four-electron terms in the product of (7.7a) and (7.7b) and adding the partial results.

Thus far we have considered effective operators formed from the product of curtailed operators both of which are of the type (3.12). Each curtailed operator (7.7a) and (7.7b) is a sum of two distinct interaction graphs. For any pair of graphs in the product [e.g., the pair in (7.8)] the three- and two-electron parts were formed by contracting the pair in a unique way [e.g., by putting $j=r$ to obtain (7.9)]. However, when curtailed operators of the type (3.16) or (3.19), which have a pair of electrons on the left or right with the same subshell labels, occur, there may be more than one

contraction leading to the same three- or two-electron term. Furthermore, curtailed operators of the form (3.19) have an additional weight factor $\frac{1}{2}$. In these cases it is obviously desirable to compute at the outset the weight of each distinct type of n -electron graph, aside from the weight factor (7.13), which arises from the summation $i \neq j \neq \dots$. Rather than attempt to give a prescription for these weight factors, we will indicate the procedure to be followed by considering a specific example.

We consider a term in the summation (7.5) of the type $\bar{P}(\lambda\lambda\lambda'; \lambda'\lambda'\pi\pi)$ which is the matrix element of the effective operator $\bar{V}(\lambda\lambda, \lambda'\lambda')\bar{V}(\lambda'\lambda', \pi\pi)$. The curtailed operators are both of the form (3.19), i.e.,

$$\bar{V}(\lambda\lambda, \lambda'\lambda') = \frac{1}{2} \sum_{i \neq j} \sum_{k} \begin{array}{c} i \text{---} \lambda \text{---} \bigcirc \text{---} \lambda' \text{---} i \\ | \\ \times k \\ | \\ j \text{---} \lambda \text{---} \bigcirc \text{---} \lambda' \text{---} j \end{array} \quad (7.15a)$$

and

$$\bar{V}(\lambda'\lambda', \pi\pi) = \frac{1}{2} \sum_{r \neq s} \sum_{k'} \begin{array}{c} r \text{---} \lambda' \text{---} \bigcirc \text{---} \pi \text{---} r \\ | \\ \times k' \\ | \\ s \text{---} \lambda' \text{---} \bigcirc \text{---} \pi \text{---} s \end{array} \quad (7.15b)$$

The four-electron part of the product of (7.15a) and (7.15b) does not involve contraction but comes from terms in which $(i, j) \neq (r, s)$, i.e., the four-electron part is the operator

$$\frac{1}{4} \sum_{i \neq j \neq r \neq s} \sum_{kk'} \begin{array}{c} i \text{---} \lambda \text{---} \bigcirc \text{---} \lambda' \text{---} i \\ | \\ \times k \\ | \\ j \text{---} \lambda \text{---} \bigcirc \text{---} \lambda' \text{---} j \\ | \\ r \text{---} \lambda' \text{---} \bigcirc \text{---} \pi \text{---} r \\ | \\ \times k' \\ | \\ s \text{---} \lambda' \text{---} \bigcirc \text{---} \pi \text{---} s \end{array} \quad (7.16)$$

In the matrix element of (7.16), the summation over $i \neq j \neq r \neq s$ leads to the weight factor F_n^m given by (7.13) so that in this case the total weight is $F_n^m/4$.

To obtain three-electron terms in the product of (7.15a) and (7.15b) we can contract either of the lines labeled i, j on the right of (7.15a) with either of the lines labeled r, s on the left of (7.15b). This gives four terms corresponding to $i=r, i=s, j=r, j=s$. However, since the graphs in (7.15a) and (7.15b) can be rotated through 180° about a horizontal axis in the plane of the paper without changing their matrix elements and since each summation is symmetric in its indices, one can see that each of the 4 three-electron terms will be equal. Consequently we need consider just one term, say that with $j=r$ and cancel the factor $\frac{1}{4}$. Then the three-electron part is given by

$$\sum_{i \neq j \neq s} \sum_{kk'} \begin{array}{c} i \text{---} \lambda \text{---} \bigcirc \text{---} \lambda' \text{---} i \\ | \\ \times k \\ | \\ j \text{---} \lambda \text{---} \bigcirc \text{---} \lambda' \text{---} \pi \text{---} j \\ | \\ \times k' \\ | \\ s \text{---} \lambda' \text{---} \bigcirc \text{---} \pi \text{---} s \end{array} \quad (7.17)$$

Again, the summation $i \neq j \neq s$ contributes the weight factor (7.13) to the matrix element of (7.17).

Finally, there are 2 two-electron terms in the product of (7.15a) and (7.15b) corresponding to $i=r, j=s$ or $i=s, j=r$. Clearly these two terms are not distinct, so that we need consider only one of them and cancel one factor $\frac{1}{2}$, i.e., the two-electron part is

$$\frac{1}{2} \sum_{i \neq j} \sum_{kk'} \begin{array}{c} i \text{---} \lambda \text{---} \bigcirc \text{---} \lambda' \text{---} i \\ | \\ \times k \\ | \\ j \text{---} \lambda \text{---} \bigcirc \text{---} \lambda' \text{---} \pi \text{---} i \\ | \\ \times k' \\ | \\ j \text{---} \lambda \text{---} \bigcirc \text{---} \lambda' \text{---} \pi \text{---} j \end{array} \quad (7.18)$$

Perturbation terms which contain a multipole interaction matrix element occur in the theory of crystal field interactions (RW64) and in perturbation corrections to the dipole matrix element in the calculation of photoionization cross sections (MB65, CM68). In this

case the product of curtailed operators such as appears in (7.4) contains a multipole operator of the type (5.11). Again the n -electron terms of the effective operator are obtained by performing all possible contractions of the product of curtailed operator graphs. Each graph is then contracted with the state graphs to give a contribution to the perturbation term of the type (7.12). However, in this case the diagram contains a free k line. This diagram is evaluated by the procedure which was used in Sec. 5.2 for the single multipole matrix element.

The foregoing procedure for the evaluation of perturbation terms like (7.1) can be summarized by the following sequence of operations:

(i) For each matrix element, identify and list the possible sets of interacting subshells according to step (i) of Sec. 6.1. Replace each Coulomb operator by the sum of the curtailed operators, i.e.,

$$\sum_{i < j} V_{ij} \rightarrow \sum_{(\lambda\mu\lambda'\mu')} \bar{V}(\lambda\mu, \lambda'\mu'), \quad (7.19)$$

where $\bar{V}(\lambda\mu, \lambda'\mu')$ is of the form (3.12), (3.16), or (3.19). A multipole interaction operator is replaced by the sum of curtailed operators (5.11). The matrix element of each term in the product of operators like the right-hand side of (7.19) can be evaluated separately. For each term, proceed as in the next step.

(ii) Express the product of curtailed operators as a sum of n -electron interaction graphs by contracting corresponding free lines as was done in steps (1)–(3) above for the product of (7.7a) and (7.7b). Where curtailed operators of the type (3.16) or (3.19) appear, compute the weight of each *distinct* n -electron graph as was done in (7.16)–(7.18). This procedure gives the sum over electron labels in the form $i \neq j \neq r \dots$ for each graph. At this stage the electron labels i, j , etc, may be omitted and the summation over them removed from each graph. This summation is replaced by the weight factor (7.13) in step (viii) of this prescription.

The matrix element of each n -electron graph is obtained by drawing the graph with the free lines ordered vertically downwards according to the subshell ordering and then following steps (iii)–(xi) of Sec. 6.1.

Steps (ii)–(xi) are then repeated for all other terms of the effective operator obtained in step (i) and the partial results added.

7.2 Example

The procedure of Sec. 7.1 will be illustrated by the evaluation of certain terms contributing to the perturbation of states of the configuration $(nl)^N$ outside closed shells. This example is chosen for comparison with previous work on effective operators (RW63, RS67). We also make contact with the work of Judd

(J67), who listed the interaction graphs which contribute to the perturbation of the configuration $(nl)^N$.

Specifically we will treat the perturbation of the configuration (closed shells $+\rho^N\sigma^N\sigma'$) by the configuration (closed shells $+\rho^{N\rho-1}\sigma^N\sigma\rho'$). In the state which is perturbed, the subshell ρ is closed, i.e., $N_\rho = 4l_\rho + 2$. We will ignore interactions other than those between the subshells ρ, σ , and ρ' , on the assumption that interactions with closed shells are canceled in the perturbation by matrix elements of the potential used to define the one-electron basis. See J67 for a discussion of this point.

We wish to evaluate the second-order perturbation

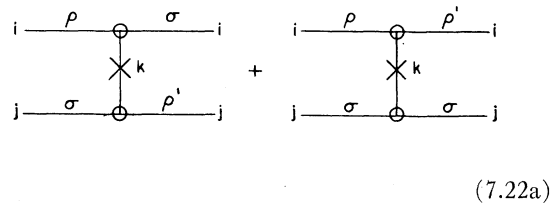
$$P = (1/\Delta E) \sum_{\beta} (\rho^N\sigma^N\sigma', \alpha LS | \sum_{i < j} V_{ij} | \rho^{N\rho-1}\sigma^N\sigma\rho', \beta LS) \\ \times (\rho^{N\rho-1}\sigma^N\sigma\rho', \beta LS | \sum_{r < s} V_{rs} | \rho^N\sigma^N\sigma', \alpha' LS). \quad (7.20)$$

Step (i). For the first matrix element there is a single set of interacting subshells $\{\rho\sigma, \sigma\rho'\}$ with the spectator electron configuration

$$\bar{N}_\rho = N_\rho - 1, \quad \bar{N}_\sigma = N_\sigma - 1, \quad \bar{N}_{\rho'} = 0. \quad (7.21)$$

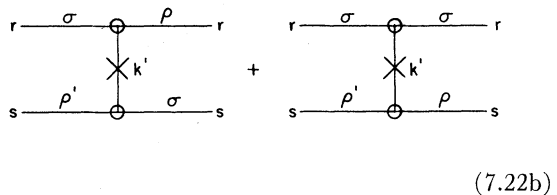
Similarly, in the second matrix element there is a single set $\{\sigma\rho', \rho\sigma\}$ with the spectator electron configuration (7.21). The curtailed operators are

$$\bar{V}(\rho\sigma, \sigma\rho') = \sum_k \sum_{i \neq j}$$



for the first matrix element and

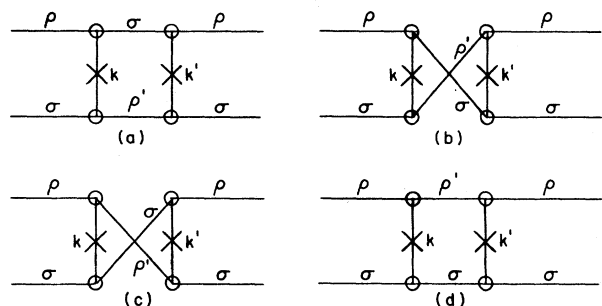
$$\bar{V}(\sigma\rho', \rho\sigma) = \sum_{k'} \sum_{r \neq s}$$



for the second matrix element.

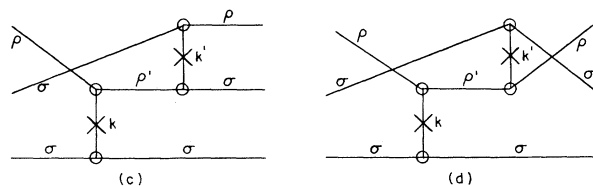
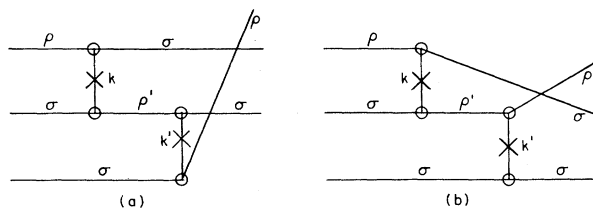
Step (ii). In the product of (7.22a) and (7.22b), contraction of the σ and ρ' lines gives four distinct graphs. These are the only two-electron graphs. Consequently, the two-electron interaction is the sum of

the matrix elements of the graphs



(7.23)

There are four distinct three-electron graphs obtained by contracting only the ρ' lines in each pair of graphs in the product of (7.22a) and (7.22b). These four graphs are the only three-electron graphs. The three-electron interaction is obtained by adding the matrix elements of the graphs



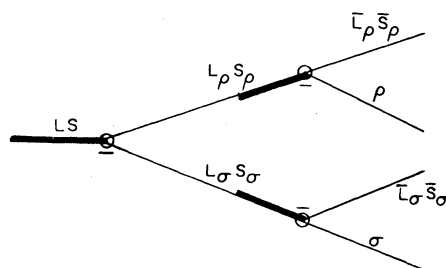
(7.24)

Since the subshell ρ' is unoccupied in the perturbed state, the contribution of all four-electron graphs (i.e., pairs of graphs with no lines contracted) is zero. To obtain P in (7.20) the matrix elements of the eight graphs (7.23) and (7.24) must be evaluated and the

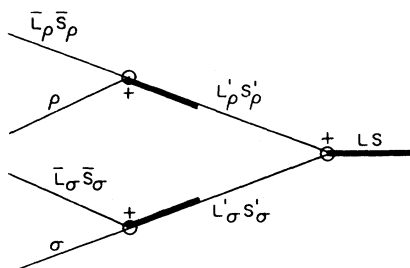
results added. We will consider as example only one graph of each class, say (7.23c) and (7.24b). The contribution of each graph is obtained by following steps (iii)-(x) of Sec. 6.1. First we consider graph (7.23c), whose matrix element we will denote by P_2 (7.23c).

Step (iii). There is a single crossing of one-electron lines so that the graph is multiplied by a factor (-1) .

Step (iv). The state graphs are



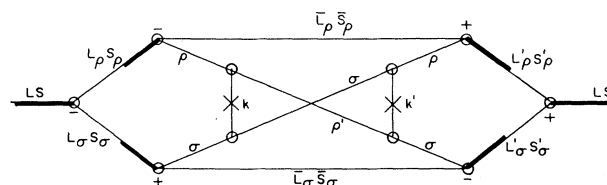
for the left-hand state and



for the right-hand state. Since the coupling schemes α, α' are trivial in this case, they have been specified in (7.25) and (7.26).

Step (v). Contraction of (7.23c) with (7.25) and (7.26) gives the diagram

$(-1) \times$

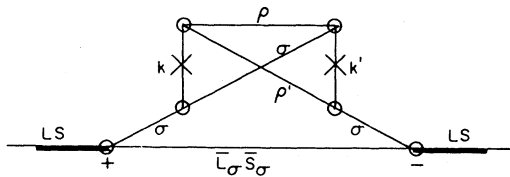


An important simplification can be made at this

point. Since the ρ subshell is closed, we have $L_\rho = L_{\rho'} = 0$, $S_\rho = S_{\rho'} = 0$. This means that the corresponding lines in the diagram (7.27) and the nodes at their ends may be removed. The removal of the nodes involving the LS lines in (7.27) follows from the relation (4.22). The removal of the two nodes involving the ρ lines gives a single ρ line from the relation

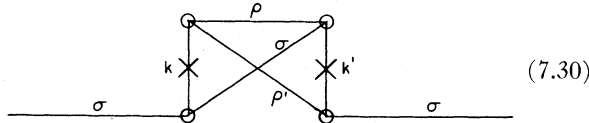
$$\sum_{\bar{M}_\rho} (00 | \bar{L}_\rho \bar{M}_\rho l_\rho m_\rho) (\bar{L}_\rho \bar{M}_\rho l_{\rho'} m_{\rho'} | 00) = [l_\rho]^{-1} \delta(l_\rho l_{\rho'}) \delta(m_\rho m_{\rho'}) \quad (7.28)$$

and a similar relation involving the corresponding spin momenta. In this way the diagram (7.27) becomes



$$\times [- ([\frac{1}{2}] [l_\rho])^{-1} \delta(L_\sigma L) \delta(S_\sigma S) \times \delta(L_\sigma' L) \delta(S_\sigma' S)] \quad (7.29)$$

This simplification has been performed at this stage to demonstrate that the two-electron interaction graph (7.23c) can be represented by the *one-electron* effective operator



In other words, when an electron is excited out of a closed subshell on the right and an electron falls into a single hole in the same subshell on the left, we may contract the corresponding lines. This condition holds for all the ρ lines in (7.23) and (7.24). This means that all the two-electron graphs represent effective one-electron operators of the type (7.30) and, as we shall see, all the three-electron graphs (7.24) reduce to two-electron effective operators. The factor $([\frac{1}{2}] [l_\rho])^{-1}$ introduced by removal of nodes is equal to N_ρ^{-1} .

Steps (vi) and (vii) give the expression

$$- ([\frac{1}{2}] [l_\rho])^{-1} \sum_{kk'} (-1)^{k'} X(k; \rho\sigma\rho'\sigma) X(k'; \rho'\sigma\rho\sigma) \times \sum_{\bar{L}_\sigma \bar{S}_\sigma} (l_\sigma^{N_\sigma} \alpha LS \{ | l_\sigma^{N_\sigma-1} \bar{L}_\sigma \bar{S}_\sigma l_\sigma \} \times (l_\sigma^{N_\sigma-1} \bar{L}_\sigma \bar{S}_\sigma l_\sigma \{ | l_\sigma^{N_\sigma} \alpha' LS \} \times \mathcal{G} \quad (7.31)$$

where \mathcal{G} is the diagram (7.29) with the crosses on the k, k' lines removed: k has even values only.

Step (viii). The weight factor is

$$(N_\rho N_\sigma N_\rho N_\sigma)^{1/2} = N_\rho N_\sigma \quad (7.32)$$

The factor N_ρ in (7.23) cancels the factor N_ρ^{-1} introduced in step (iv), in accordance with the fact that the effective operator (7.30) transfers electrons from the σ subshell only. This means that we can use the simplified form (7.30) of the interaction graph from the outset of step (iv).

Step (ix). In the Pauli phase factor,

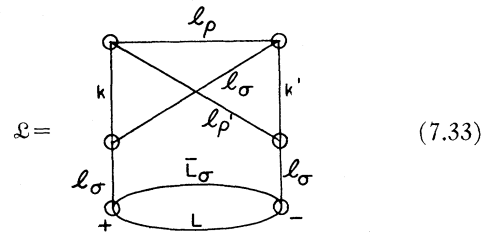
$$P_A = N_\sigma - 1$$

and

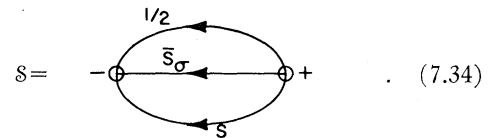
$$P_{A'} = N_\sigma - 1,$$

so that the Pauli phase is +1.

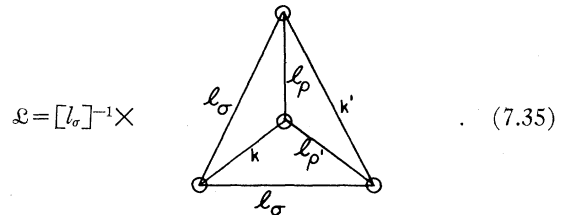
Step (x). Application of steps (i)-(v) of Sec. 4 to the diagram in (7.29) gives the result $\mathcal{G} = \mathcal{L} \times \mathcal{S}$, where



and



The orbital diagram, after removal of the closed loop according to (4.24), can be drawn in the form



The diagram in (7.35) is the 6-*j* coefficient

$$\begin{Bmatrix} k & l_{\rho'} & l_{\rho} \\ k' & l_{\sigma} & l_{\sigma} \end{Bmatrix}.$$

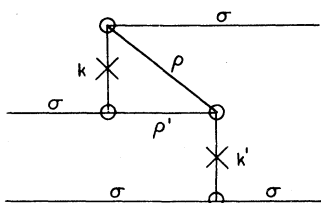
The spin diagram \mathcal{S} is the unit diagram $\Delta(\bar{S}_{\sigma\frac{1}{2}}\mathcal{S})$. These results mean that the factor \mathcal{G} in (7.31) is independent of any quantum numbers appearing in the c.f.p. Consequently, the sum over the c.f.p. gives the factor $\delta(\alpha\alpha')$ by closure. Finally we have the result

$$P_2(7.23c) = -(N_{\sigma}/[L_{\sigma}])\delta(\alpha\alpha') \times \sum_{kk'} X(k; \rho\sigma\rho'\sigma)X(k'; \rho'\sigma\rho\sigma)(-1)^{k'} \times \begin{Bmatrix} k & l_{\rho'} & l_{\rho} \\ k' & l_{\sigma} & l_{\sigma} \end{Bmatrix}. \quad (7.36)$$

We now consider graph (7.24b), whose matrix element we denote by P_3 (7.24b). We repeat steps (iii)-(x) of Sec. 6.1.

Step (iii). There is a single crossing of 1-electron lines which gives a factor (-1) . We will make the simplification used to derive (7.30) from (7.23c) to convert (7.24b) to a 2-electron interaction graph, i.e. since the ρ subshell is closed in both left-hand and right-hand configurations we can contract the two ρ lines in (7.24b) to give

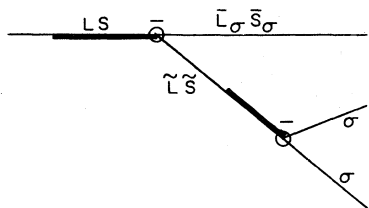
$(-1) \times$



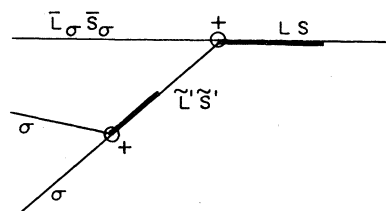
(7.37)

We will use this form henceforth: however, the factor (-1) must be included from step (iii) *before* contracting the ρ lines.

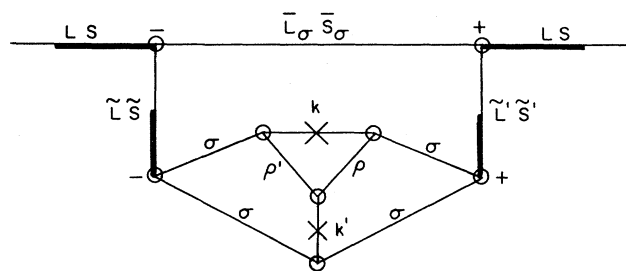
Step (iv). The state graph for the left-hand wave function is



and for the right-hand wave function



Step (v). Contraction of the two state graphs with the interaction graph (7.37) gives the diagram



(7.38)

Steps (vi) and (vii) give the expression

$$(-) \sum_{kk'} X(k; \rho\sigma\rho'\sigma)X(k'; \rho'\sigma\rho\sigma)(-1)^{k+k'} \times \sum_{f.p.} (l_{\sigma}^{N_{\sigma}}LS\{|\bar{L}_{\sigma}\bar{S}_{\sigma}l_{\sigma}^2\bar{L}\bar{S}\rangle\langle\bar{L}_{\sigma}\bar{S}_{\sigma}l_{\sigma}^2\bar{L}'\bar{S}'|\}l_{\sigma}^{N_{\sigma}}LS) \times \mathcal{G}, \quad (7.39)$$

where \mathcal{G} is the diagram in (7.38) with the crosses removed.

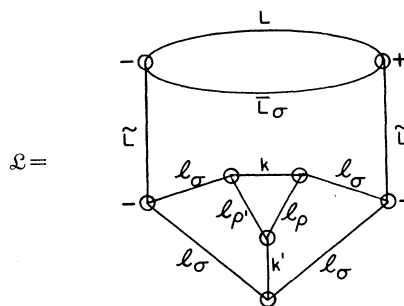
Step (viii). The weight factor is $N_{\sigma}(N_{\sigma}-1)$.

Step (ix). The Pauli phase factor has

$$P_A = P_B = 0$$

giving a phase of $+1$.

Step (x). Application of steps (i)-(v) of Sec. 4 to the diagram in (7.32) gives $\mathcal{G} = \mathcal{L} \times \mathcal{S}$, where



$\times ([\bar{L}][\tilde{L}'])^{1/2}$ (7.40)

and

$$S = \times ([\tilde{S}][\tilde{S}'])^{1/2}. \quad (7.41)$$

After removal of the closed loop, the orbital diagram may be separated on the three lines l_σ, k', l_σ to give

$$\mathcal{E} = \delta(\tilde{L}\tilde{L}'). \quad (7.42)$$

Since k' is even, we have the result

$$\mathcal{E} = (-1)^{\tilde{L}} \begin{Bmatrix} k' & l_\rho & l_{\rho'} \\ k & l_\sigma & l_\sigma \end{Bmatrix} \times \begin{Bmatrix} k' & l_\sigma & l_\sigma \\ \tilde{L} & l_\sigma & l_\sigma \end{Bmatrix} \delta(\tilde{L}\tilde{L}'). \quad (7.43)$$

The spin diagram reduces to the unit diagram, i.e.,

$$S = \delta(\tilde{S}\tilde{S}') \Delta(\frac{1}{2}\tilde{S}). \quad (7.44)$$

The final result is then

$$P_3(7.24b) = -N_\sigma(N_\sigma - 1) \times \sum_{kk'} X(k; \rho\sigma\sigma\rho') X(k'; \rho'\sigma\rho\sigma) (-1)^k \begin{Bmatrix} k' & l_\rho & l_{\rho'} \\ k & l_\sigma & l_\sigma \end{Bmatrix} \times \sum_{\tilde{L}\tilde{L}\tilde{S}} (l_\sigma^{N_\sigma} LS \{ | \tilde{L}_\sigma \tilde{S}_\sigma l_\sigma^2 \tilde{L} \tilde{S} \} (\tilde{L}_\sigma \tilde{S}_\sigma l_\sigma^2 \tilde{L} \tilde{S} \{ | l_\sigma^{N_\sigma} LS \} \times (-1)^{\tilde{L}} \begin{Bmatrix} k' & l_\sigma & l_\sigma \\ \tilde{L} & l_\sigma & l_\sigma \end{Bmatrix}. \quad (7.45)$$

Finally, we compare the results obtained here with other treatments of the perturbation term (7.20). After contraction of the ρ lines, the 4 two-electron graphs (7.23) become one-electron graphs of the type C_1 and C_2 listed in Chapter 4 of Judd (J67). Again after contraction of the ρ lines, the 4 three-electron graphs

(7.24) are the two-electron graphs $F_1, F_2, F_3,$ and F_4 of Judd.

The graph (7.23b) is of the same structure as (7.23c) and one can show that its matrix element is given by (7.36), except that k and k' are interchanged, which does not alter its value. Similarly, the graph (7.24c) is of the same structure as (7.24b) and again one can show that their matrix elements are the same, i.e., $P_3(7.24c) = P_3(7.24b)$.⁶ The sum $P_2(7.23b) + P_2(7.23c)$ and the sum $P_3(7.24b) + P_3(7.24c)$ are the one- and two-electron parts, respectively, of the term C_3 given in Eq. (61) of Racah and Stein (RS67).

8. GENERAL FORM OF THE MATRIX ELEMENT

In this section we will indicate how the particular interaction operators (3.1), (5.2), and (7.4) which we have considered, form part of a general scheme for the evaluation of interaction matrix elements from a graphical representation of the angular factor. The essential point is that any coupled product of tensor operators may be represented by a graph. By use of the transformation (2.4), each one-electron operator gives rise to the graph of a C-G coefficient involving a free k line. The operator graph is assembled by coupling the free k lines according to the coupling scheme of the operator product. The matrix element is then represented by bracketing the n -electron operator graph with the graphs of the N -electron wave functions. The point which must be emphasized is that this graphical representation of the interaction operator separates the process of antisymmetrization from the recoupling of angular momentum. The antisymmetrization of wave functions gives rise to a weight factor and a Pauli phase factor, which depend only upon the number and location of the interacting electrons. Hence, the complexity of the general form of the interaction operator arises mainly in the coupling of angular momentum, i.e., in the \mathcal{G} diagram.

8.1 Graphical Representation

In the following, we shall show how the graphical representation of any interaction operator is obtained and indicate the broader application of the methods of preceding sections, but we will not attempt to give detailed procedures for the wide variety of operators which occurs in practice.

The general form of the interaction operator is

$$\sum_{t \neq u \neq \dots} f(r_t, r_u, \dots) [K_t, K_u, \dots, \beta]_Q^{[K]}. \quad (8.1)$$

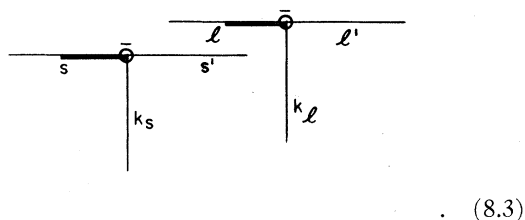
Here, $f(r_t, r_u, \dots)$ represents the radial part of the operator and K_i denotes the rank of a tensor operator acting in the space of electron i . In general, both an

⁶ Note that the graphs (7.23b) and (7.23c) and the graphs (7.24b) and (7.24c) nevertheless are *distinct* within the meaning of section (7.1). The equality of their matrix elements is "accidental" in that it arises because (7.23b) and (7.24b) are the respective mirror images of (7.23c) and (7.24c) and the same configuration A occurs on both sides of the matrix elements.

orbital operator $L^{[k_l]}(i)$ and a spin operator $S^{[k_s]}(i)$ will operate in the space of electron i . Their components are transformed using (2.4), i.e.,

$$\begin{aligned}
 &L_q^{[k_l]} S_{q'}^{[k_s]} \\
 &= \sum_{lm_l m_s} \sum_{l'm_l' m_s'} (\Omega_i \Sigma_i | l s m_l m_s) (l m_l | L_q^{[k_l]} | l' m_l') \\
 &\quad \times (s m_s | S_{q'}^{[k_s]} | s' m_s') (l' s' m_l' m_s' | \Omega_i \Sigma_i) \\
 &= \sum_{lm_l m_s} \sum_{l'm_l' m_s'} (\Omega_i \Sigma_i | l s m_l m_s) (l || L^{[k_l]} || l') \\
 &\times (s || S^{[k_s]} || s') (-1)^{2k_l+2k_s} [l]^{-1/2} [s]^{-1/2} (l m_l | l' m_l' k_l q) \\
 &\quad \times (s m_s | s' m_s' k_s q') (l' s' m_l' m_s' | \Omega_i \Sigma_i). \quad (8.2)
 \end{aligned}$$

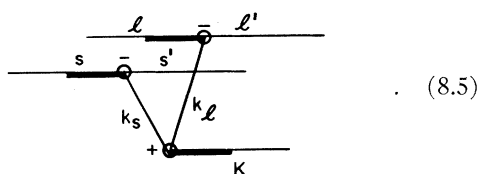
The two C-G coefficients in (8.2) are represented graphically by



In the simplest case the spin and orbital parts are uncoupled (as for the Coulomb operator, where $k_s=0$). Where the spin and orbital parts of the operator acting in the space of particle i are coupled, as in the operator

$$\Gamma[L^{[k_l]} \times S^{[k_s]}]_q^{[K]} = \sum_{q, q'} L_q^{[k_l]} S_{q'}^{[k_s]} (k_l q k_s q' | K q), \quad (8.4)$$

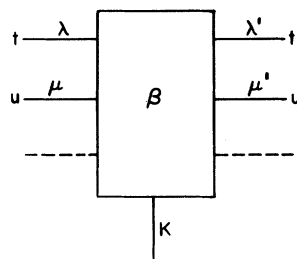
the graphical representation is



As in Sec. 2.1, the complete representation of the interaction operator is obtained by applying the expansion (8.2) to each one-electron operator, extending the summation over *all* one-electron quantum numbers, and performing the radial integration to obtain

$$\begin{aligned}
 &\sum_{t \neq u \neq \dots} f(r_t, r_u, \dots) [K_t, K_u, \dots, \beta]_q^K \\
 &= \sum_{t \neq u \neq \dots} \sum_{\lambda \mu \dots} \sum_{\lambda' \mu' \dots} R \times \{ ((-1)^{2k_l+2k_s} ([l_\lambda][s_\lambda])^{-1/2} \\
 &\quad \times (l_\lambda || L^{[k_l]}(t) || l_{\lambda'}) (s_\lambda || S^{[k_s]}(t) || s_{\lambda'}) \dots \} \times \mathcal{K}, \quad (8.6)
 \end{aligned}$$

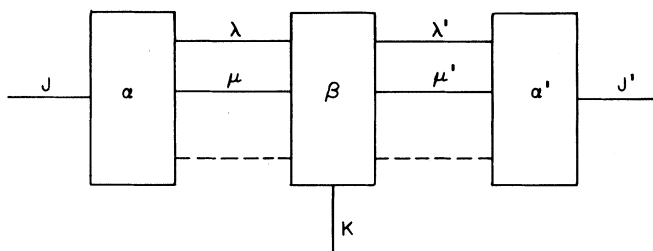
where R is the radial integral and \mathcal{K} is the n -electron operator graph



(8.7)

Here, the block β represents the coupling of the free k lines in n graphs like (8.3) or (8.5). The graphs (2.9), (2.10), and (7.8)–(7.10) are particular examples of the form (8.7).

The matrix element of each term in the sum over $\lambda u \dots \lambda' u' \dots$ in (8.6) is obtained by bracketing the appropriate graph (8.7) with wave function graphs like (2.15) and contracting corresponding free lines. The result can always be written as a product of a weight factor, a Pauli phase factor, and a \mathcal{G} diagram. In addition, there will be the appropriate integrals involving one-electron quantum numbers from (8.7) and a possible summation over fractional parentage. The \mathcal{G} diagram is of the form



(8.8)

where the lines λ , etc., now represent both the orbital lines l_λ and spin lines s_λ .

8.2 Evaluation of the Matrix Element

The \mathcal{G} diagram is evaluated by the procedure of Sec. 4. Where an L - S scheme of coupling is used, it is

usually possible to separate the diagram into a diagram containing the spin interaction, a diagram containing the orbital interaction, and a diagram involving only "total" angular momenta. Bordarier (Bo70) has given a comprehensive discussion of the separation of \mathcal{J} diagrams involving L - S coupling schemes. Where j - j coupling is used the one-electron lines l_λ, s_λ , etc., which issue from the operator block are coupled to resultant j_λ , etc., in the wave function blocks α, α' . Hence, it is not possible in general to separate spin and orbital recoupling.

The Pauli phase factor which arises from the shift of interacting electrons from the standard order can be obtained from the procedure of (F65) as used in previous sections. The weight factor arising from the summation $l \neq u \neq \dots$ is independent of the coupling scheme used and is given by (7.13).

We have briefly indicated the general scheme of matrix element evaluation by the use of graphs, of which the matrix elements treated in previous sections are particular examples. Bordarier (Bo70) has given further specific examples of the application of these techniques to the matrix elements of other interaction operators.

ACKNOWLEDGMENTS

I am deeply indebted to Professor U. Fano for numerous discussions which clarified many aspects of the formulation, for his editorial advice and active assistance with details of the graphical method, particularly Secs. 2 and 4, and not least for his encouragement during the course of this work. I am grateful also to Dr. J. Sugar for suggesting the example of Sec. 6 and for helpful correspondence, and to Dr. Y-K. Kim and A. F. Starace for critical reading of the manuscript.

REFERENCES

- A68 L. Armstrong, Jr., Phys. Rev. **172**, 12 (1968).
 B70 P. G. Burke, Comp. Phys. Comm. **1**, 241 (1970).
 BG34 R. F. Bacher and S. Goudsmit, Phys. Rev. **46**, 948 (1934).
 Bo70 Y. Bordarier, thesis, University of Paris, 1970.
 Br70 J. S. Briggs, J. Math. Phys. **11**, 1198 (1970).
 BS68 D. M. Brink and G. R. Satchler, *Angular Momentum* (Oxford U. P., Oxford, 1968), 2nd ed.
 CM68 E. S. Chang and M. R. C. McDowell, Phys. Rev. **176**, 126 (1968).
 CS35 E. U. Condon and G. H. Shortley, *Theory of Atomic Spectra* (Cambridge U. P., New York, 1935).
 E69 E. El-Baz, *Traitement Graphique de l'Algèbre des Moments Angulaires* (Masson, Paris, 1969).
 F65 U. Fano, Phys. Rev. **140**, A67 (1965).
 FP63 —, and F. Prats, Proc. Natl. Acad. Sci. India **33A**, 55s (1963).
 FPG63 —, F. Prats, and Z. Goldschmidt, Phys. Rev. **129**, 2643 (1963).
 FR59 —, and G. Racah, *Irreducible Tensorial Sets* (Academic, New York, 1959).
 J63 B. R. Judd, *Operator Techniques in Atomic Spectroscopy* (McGraw-Hill, New York, 1963).
 J67 —, *Second Quantization and Atomic Spectroscopy* (Johns Hopkins, Baltimore, 1967).
 MB65 A. Yu. Matulis and A. A. Bandzaitis, Liet. Fizik. Rinkiny. **5**, 453 (1965).
 MEL67 J.-N. Massot, E. El-Baz, and J. LaFoucrière, Rev. Mod. Phys. **39**, 288 (1967).
 MS68 D. H. Menzel and B. W. Shore, *Principles of Atomic Spectra* (Wiley, New York, 1968).
 R42a G. Racah, Phys. Rev. **61**, 186, (1942).
 R42b G. Racah, Phys. Rev. **62**, 438 (1942).
 R43 G. Racah, Phys. Rev. **63**, 367 (1943).
 RBMW59 M. Rotenberg, R. Bivins, N. Metropolis, and J. K. Wooten, Jr., *The 3-j and 6-j Symbols*, (Technology, Cambridge, Mass., 1959).
 RMY65 P. D. Rumsas, A. A. Bandzaitis, and A. P. Yutsis, Liet. Fiz. Rink. **5**, 197 (1965).
 RS67 G. Racah and J. Stein, Phys. Rev. **156**, 58 (1967).
 RW63 K. Rajnak and B. G. Wybourne, Phys. Rev. **132**, 280 (1963).
 S69 P. G. H. Sandars, Advan. Chem. Phys. **14**, 365 (1969).
 Se66 M. J. Seaton, Proc. Phys. Soc. (London) **88**, 801 (1966).
 SM68 K. Smith and L. A. Morgan, Phys. Rev. **165**, 110 (1968).
 deST63 A. de-Shalit and I. Talmi, *Nuclear Shell Theory* (Academic, New York, 1963).
 T69 V. V. Tolmachev, Advan. Chem. Phys. **14**, 471 (1969).
 W68 B. G. Wybourne, J. Chem. Phys. **48**, 2596 (1968).
 YB65 A. P. Yutsis and A. A. Bandzaitis, *Teoriia Momenta Kolichestva Dvizheniia v Kvantovoi Mekhanike* (Lietuvos TSR Mokslo Akademija, Vilna, 1965).
 YLV62 A. P. Yutsis, I. B. Levinson, and V. V. Vanagas, *The Theory of Angular Momentum* (Israel Program for Scientific Translations, Jerusalem, 1962).